

WANL-PR(Q)-008

NASA-CR-54894

FACILITY FORM 002

N66-23864

(ACCESSION NUMBER)

26

(PAGES)

CR-54894

(NASA CR OR TMX OR AD NUMBER)

(THRU)

1

(CODE)

17

(CATEGORY)

DEVELOPMENT OF DISPERSION STRENGTHENED TANTALUM BASE ALLOY

Seventh Quarterly Report

by

R.W. Buckman and R.C. Goodspeed

prepared for

National Aeronautics and Space Administration

Lewis Research Center

Space Power Systems Division

Under Contract (NAS 3-2542)



GPO PRICE \$ _____

CFSTI PRICE(S) \$ _____

Hard copy (HC) 3.00

Microfilm (MF) .75

Astronuclear Laboratory
Westinghouse Electric Corporation

653 July 65

NOTICE

This report was prepared as an account of Government-sponsored work. Neither the United States nor the National Aeronautics and Space Administration (NASA), nor any person acting on behalf of NASA:

- A) Makes any warranty or representation, expressed or implied, with respect to the accuracy, completeness, or usefulness of the information contained in this report, or that the use of any information apparatus, method, or process disclosed in this report may not infringe privately-owned rights; or
- B) Assumes any liabilities with respect to the use of, or for damages resulting from the use of any information, apparatus, method or process disclosed in this report.

As used above, "person acting on behalf of NASA" includes any employee or contractor of NASA, or employee of such contractor, to the extent that such employee or contractor of NASA or employee of such contractor prepares, disseminates, or provides access to, any information pursuant to his employment or contract with NASA, or his employment with such contractor.

Copies of this report can be obtained from:

National Aeronautics & Space Administration
Office of Scientific and Technical Information
Washington 25, D. C.
Attention: AFSS-A

**DEVELOPMENT OF DISPERSION STRENGTHENED
TANTALUM BASE ALLOY**

by
R. W. Buckman, Jr.
and
R. C. Goodspeed

**SEVENTH QUARTERLY PROGRESS REPORT
Covering the Period**

May 20, 1965 to August 20, 1965

**Prepared For
NATIONAL AERONAUTICS AND SPACE ADMINISTRATION
Contract NAS 3-2542**

**Technical Management
Paul E. Moorhead
NASA-Lewis Research Center
Space Power Systems Division**

**Astronuclear Laboratory
Westinghouse Electric Corporation
Pittsburgh 36, Pa.**

23864
ABSTRACT

Development of dispersion strengthened tantalum base alloys for use in advanced space power systems continued with the processing of the upset forged ingot of NASV-20 (Ta-8W-1Re-0.7Hf-0.025C) to 0.040 inch sheet. Evaluation of this material was initiated. The seventh and final optimized composition was melted and processed. Evaluation of these alloys was also completed. Phase identification and morphology studies were continued using optical and electron microscopy and x-ray and electron diffraction techniques.

TABLE OF CONTENTS

	<u>Page No.</u>
I. INTRODUCTION	1
II. PROGRAM STATUS	2
A. OPTIMIZATION INVESTIGATION	2
B. FOUR INCH DIAMETER INGOT SCALE-UP	24
C. TURBINE COMPOSITIONS	36
D. PHASE IDENTIFICATION AND MORPHOLOGY	38
III. FUTURE WORK	43
IV. REFERENCES	44
APPENDIX I	45
APPENDIX II	47

LIST OF TABLES

	<u>Page No.</u>
1. Melting Data for Composition NASV-18	2
2. Forging Data for Compositions NASV-17 and NASV-18	3
3. Diamond Pyramid Hardness Data for Compositions NASV-12 through NASV-18	4
4. Chemical Analyses of Compositions NASV-12 through NASV-18	6
5. Microstructure and Room Temperature Hardness After Annealing As-Rolled 0.06 Inch Sheet for One Hour	7
6. Ductile-Brittle Transition Temperatures of Compositions NASV-16, NASV-17, and NASV-18	8
7. Summary of Ductile-Brittle Transition Temperature Data for Optimization Compositions	10
8. Mechanical Properties of Compositions NASV-12 through NASV-18	14
9. Creep Properties of Optimized Tantalum Alloys at 1×10^{-8} Torr	17
10. Forging Data for Composition NASV-20	27
11. Chemical Analysis of Composition NASV-20	29
12. Ductile-Brittle Transition Temperature of Composition NASV-20	30
13. Mechanical Properties of Composition NASV-20	31
14. Diamond Pyramid Hardness Data for Composition NASV-15	37
15. Chemical Analysis of Composition NASV-15	37
16. Room Temperature Tensile Data on Composition NASV-11	37
17. X-Ray Diffraction Analyses on Extracted Residues from Compositions NASV-10, NASV-11, and NASV-15	41

LIST OF FIGURES

	<u>Page No.</u>
1. Effect of Interstitial Content on the Ductile-Brittle Transition Temperature of TIG Welded Optimization Compositions	11
2. Effect of Rhenium and Equivalent Tungsten Contents on the Ductile-Brittle Transition Temperature of As-TIG Welded Optimization Compositions Tested over Bend Radius of 1.8t	12
3. Creep Properties of the Optimization Compositions Based on the Larson-Miller Parameter	19
4. Effect of Substitutional Solute Content on the Creep Behavior of the Optimization Compositions	21
5. Effect of Equivalent Tungsten Content on the Creep Behavior of the Optimization Compositions	22
6. Effect of Interstitial Content on the Creep Behavior of the Optimization Compositions	23
7. Effect of Rhenium Content on the Creep Behavior of the Optimization Compositions	25
8. Upset Forged Ingot of NASV-20	26
9. Side Forged Ingot of NASV-20	28
10. Mechanical Behavior of NASV-20 as a Function of Temperature	32
11. Creep Properties of Fabricable Tantalum Base Alloys Based on the Larson-Miller Parameter	34
12. Microstructure of As-Cast NASV-20 Showing Tantalum Dimetal Carbide Precipitate	35
13. Tantalum Rich Corner of the 1315°C Isotherm of the (Ta+W)-Hf-C Pseudo Ternary Phase Diagram	39

I. INTRODUCTION

This seventh quarterly progress report on the NASA sponsored program, "Development of a Dispersion Strengthened Tantalum Base Alloy", describes the work accomplished during the period May 20, 1965 to August 20, 1965. The work was performed under Contract NAS 3-2542.

Double vacuum arc melting of three compositions in the form of 60 pound, 4 inch diameter ingots is the primary objective of this Phase II work. These compositions are to be used for sheet and tubing applications, and will be selected for their weldability, creep resistance, and fabricability characteristics.

Prior to this quarterly period, several promising tantalum alloy compositions, which exhibited good creep resistance at 1315°C (2400°F) while maintaining adequate fabricability and weldability, were developed.¹ From these alloys, a weldable composition containing a carbide dispersion, Ta-8W-1Re-0.7Hf-0.025C (Heat NASV-20), was selected and melted as the first 4 inch diameter ingot. Seven additional 2 inch diameter ingot compositions were selected to further optimize the carbo-nitride dispersion strengthened compositions with respect to fabricability, weldability, and creep strength before selection of the remaining two 4 inch diameter ingot compositions.

During this quarterly period the NASV-20 upset forging was processed to 0.040 inch sheet and evaluation of this sheet was initiated. The seventh and final optimization alloy was melted and processing of all seven optimization alloys was completed. Evaluation of these alloys was also essentially completed. Phase identification and morphology studies continued.

II. PROGRAM STATUS

A. OPTIMIZATION INVESTIGATION

The last of the optimization compositions was double vacuum AC arc melted, and all of the optimization compositions have been processed to 0.040 inch thick sheet. They have been or are being evaluated for weldability, fabricability, and creep resistance.

Melting - The first melt electrodes of composition NASV-18 (Ta-5W-1Re-0.3Zr-0.025N)* was assembled using the standard sandwich technique.¹ This electrode was then vacuum AC arc melted into a 1-5/16 inch diameter mold. Subsequently, the resulting ingot was remelted into a 2 inch diameter mold. Melt data are recorded in Table 1. Excellent side-walls were obtained. The average diamond pyramid hardness (30 Kg load) of the as-cast ingot was 294.

TABLE 1 - Melting Data for Composition NASV-18 (Ta-5W-1Re-0.3Zr-0.025N)

Melt Number	Melt Voltage (volts)	Melt Power (kw)	Melt Rate (lbs/min)
First	22-23	45-50	2.3
Second	24	55-60	4.6

Primary Breakdown - A 3/4 inch slice was removed from the bottom of the NASV-17 (Ta-4W-3Re-0.75Hf-0.01C-0.02N) and NASV-18 ingots. These slices were dip coated with an Al-12Si alloy and satisfactorily upset forged at 1280°C (2335°F) on the Dynapak. Forging data are listed in Table 2.

The balance of the NASV-17 and NASV-18 ingots were plasma sprayed with unalloyed molybdenum and extruded at 1400°C (2550°F) to sheet bar. The reduction ratio was 4 to 1.

Hardness data for the as-forged and as-extruded material of compositions NASV-12 through NASV-18 are listed in Table 3. Also included are hardness data of the as-cast

*0.04% N intentionally added to electrode, 0.025%N analyzed in ingot.

TABLE 2 - Forging Data for Compositions NASV-17 and NASV-18

Composition	Forging Temperature (°C/°F)	Reduction (%)	Upset Constant (K _u) (a) (psi)
Ta-4W-3Re-0.75Hf- 0.01C-0.02N (NASV-17)	1280/2335	62.1	132,000
Ta-5W-1Re-0.3Zr- 0.025N (NASV-18)	1280/2335	69.6	123,000

(a) $K_u = \frac{E}{VZ}$ where

E = energy used
V = volume of material deformed
Z = empirical upset factor

TABLE 3 - Diamond Pyramid Hardness^(a) Data for Compositions NASV-12 through NASV-18

Composition	Condition ^(b)	DPH ^(a)
Ta-7.5W-1.5Re-0.5Hf -0.015C-0.015N (NASV-12)	As-cast	336
	As-forged	407
	Forged plus annealed	308
	As-extruded	394
	Extruded plus annealed	313
Ta-6.5W-2.5Re-0.3Hf -0.01C-0.01N (NASV-13)	As-cast	329
	As-forged	376
	Forged plus annealed	313
	As-extruded	371
	Extruded plus annealed	305
Ta-4W-1Mo-2Re-0.3Zr -0.015C-0.015N (NASV-14)	As-cast	315
	As-forged	413
	Forged plus annealed	308
	As-extruded	352
	Extruded plus annealed	311
Ta-9W-1.5Re-1Hf-0.06N (NASV-15)	As-cast	370
	As-forged	403
	Forged plus annealed	353
	As-extruded	398
	Extruded plus annealed	---
Ta-9.5W-0.5Re-0.25Zr -0.02C-0.01N (NASV-16)	As-cast	321
	As-forged	388
	Forged plus annealed	291
	As-extruded	323
	Extruded plus annealed	289
Ta-4W-3Re-0.75Hf-0.01C -0.02N (NASV-17)	As-cast	339
	As-forged	386
	Forged plus annealed	325
	As-extruded	384
	Extruded plus annealed	328
Ta-5W-1Re-0.3Zr-0.025N (NASV-18)	As-cast	294
	As-forged	---
	Forged plus annealed	---
	As-extruded	342
	Extruded plus annealed	298

(a) Data for 30 Kg Load

(b) All anneals were for 1 hr. at 1650°C/3000°F

materials and of the forged and extruded materials after a 1 hour anneal at 1650°C (3000°F). Evaluation of composition NASV-15 as a sheet and tubing alloy was discontinued because of its unsatisfactory secondary sheet fabricability.² All additional data for this composition is discussed in Section II-C of this report.

Chemistry - Chemical analyses results on compositions NASV-12 through NASV-14 and NASV-16 through NASV-18 are reported in Table 4. Interstitial element analyses were made on pieces of 0.040 inch thick sheet processed from extruded bar. The metallic element analyses were determined from chips machined from the as-cast ingots. With the exception of nitrogen, which was present in amounts ranging from 73 to 85 percent of that desired, the analyses of the compositions were within 10 percent of the nominal values. The nitrogen was apparently lost during melting.

Recrystallization Behavior - The 1 hour recrystallization behavior of compositions NASV-12 through NASV-14 and NASV-16 through NASV-18 is recorded in Table 5. All compositions were fully recrystallized at 1500°C (2730°F) and exhibited a grain size of 0.010 to 0.017 mm, as determined by the standard line intercept method. Recrystallization ranged from 50 to 90% complete at 1400°C (2550°F). Measurements were made on 0.06 inch thick sheet which had been reduced by approximately 75 and 90 percent in thickness for material processed from forgings and extrusions respectively.

Weldability - Electron beam (EB) and tungsten inert gas (TIG) bead-on-plate welds were satisfactorily made on 0.040 inch sheet of compositions NASV-16, 17, and 18. In each case the sheet had been processed from extruded sheet bar stock and annealed for 1 hour at 1650°C (3000°F). The ductile-brittle transition temperatures (DBTT's) of these welded sheet materials are recorded in Table 6. Also included in Table 6 is the DBTT of each composition's base metal, similarly reduced and annealed.

DBTT's of base metal, EB welded, and TIG welded material for all of the optimization compositions in the annealed (for 1 hour at $1650^{\circ}\text{C}/3000^{\circ}\text{F}$) condition were reviewed to

TABLE 4 - Chemical Analyses of Compositions NASV-12 through NASV-18

Nominal Electrode Composition	Type and Position of Sample	Analysis (Weight Percent)						
		W	Re	Mo	Hf	Zr	C	N
NASV-12 (Ta-7.5W- 1.52Re-0.5Hf- 0.015C-0.015N)	Ingot	7.9	1.52	--	0.5	--	0.019	0.011
	Sheet	--	--	--	--	--	0.016	0.011
NASV-13 (Ta-6.5W- 2.5Re-0.3Hf- 0.01C-0.01N)	Ingot	6.3	2.57	--	0.3	--	0.011	0.012
	Sheet	--	--	--	--	--	0.011	0.0085
NASV-14 (Ta-4W- 1Mo-2Re-0.3Zr- 0.015C-0.015N)	Ingot	4.0	2.05	1.01	--	0.3	0.016	0.013
	Sheet	--	--	--	--	--	0.015	0.012
NASV-16 (Ta-9.5W- 0.5Re-0.25Zr- 0.02C-0.01N)	Ingot(T&B)	9.8	0.46	--	--	0.26	--	--
	Sheet	--	--	--	--	--	0.020	0.0082
NASV-17 (Ta-4W- 3Re-0.75Hf- 0.01C-0.02N)	Ingot (B)	--	--	--	--	--	0.012	0.015
	Sheet	4.4	2.74	--	0.71	--	--	--
NASV-18 (Ta-5W- 1Re-0.3Zr- 0.04N)	Ingot (T)	4.9	1.09	--	--	0.25	--	--
	Ingot (B)	4.9	1.09	--	--	0.28	--	--
	Sheet	--	--	--	--	--	--	0.025

**TABLE 5 - Microstructure and Room Temperature Hardness After Annealing
As-Rolled 0.06-Inch Sheet for One Hour**

Composition and Heat No.	Prior Reduction Percent	As Rolled	Temperature $\frac{^{\circ}\text{C}}{^{\circ}\text{F}}$						
			1200 2190	1300 2370	1400 2550	1500 2730	1600 2910	1700 3090	1800 3270
Ta-7.5W-1.5Re- 0.5Hf-0.015C- 0.015N (NASV-12)	78.4	a)396 W	352 W	350 W	304 R50	313 RX	308 RX	310 RX	316 RX
Ta-6.5W-2.5Re- 0.3Hf-0.01C- 0.01N (NASV-13)	74.6	a)385 W	341 W	336 W	311 R50	314 RX	311 RX	303 RX	304 RX
Ta-4W-1Mo-2Re- 0.3Zr-0.015C- 0.015N (NASV-14)	76.0	a) -- --	351 W	357 W	312 R50	306 RX	309 RX	303 RX	307 RX
	88.6	b)404 W	338 W	345 RB	303 R75	313 RX	312 RX	318 RX	316 RX
Ta-9.5W-0.5Re- 0.25Zr-0.02C- 0.01N (NASV-16)	72.6	a) -- --	362 W	327 RB	285 R50	299 RX	293 RX	295 RX	293 RX
	92.0	b)397 W	360 W	282 RB	277 R75	292 RX	291 RX	297 RX	292 RX
Ta-4W-3Re-0.75Hf- 0.01C-0.02N (NASV-17)	80.1	a)438 W	381 W	346 RB	316 R90	327 RX	336 RX	330 RX	326 RX
	92.0	b)428 W	387 W	340 RB	315 R90	329 RX	333 RX	328 RX	331 RX
Ta-5W-1Re-0.3Zr- 0.025N (NASV-18)	88.6	b)378 W	352 W	295 RB	272 R75	274 RX	283 RX	286 RX	277 RX

Remarks:

W - Wrought
 RB - Recrystallization just started
 R50 - About 50% recrystallized
 R75 - About 75% recrystallized
 R90 - About 90% recrystallized
 RX - Fully recrystallized

(a) Sheet rolled from upset forging
 (b) Sheet rolled from extruded sheet
 bar

**TABLE 6 - Ductile-Brittle Transition Temperatures of Compositions
NASV-16, NASV-17, and NASV 18^(a)**

Composition and Heat No.	Condition	Temperature °F/°C	No. Load Bend Angle (degrees)	Remarks
Ta-9.5W-0.5Re- 0.25 Zr-0.02C- 0.01N (NASV-16)	Base Metal ^(b)	-200/-129	91	Bend
		-225/-143	40	Break
	Electron Beam welded ^(b)	-100/-73	91	Bend
		-125/-87	100	Break
	TIG Welded ^(b)	+75/+24	96	Bend ^(e)
		-25/-32	46	Break
Ta-4W-3Re- 0.75 Hf-0.01C- 0.02N (NASV-17)	Base Metal ^(b)	-225/-143	94	Bend
		-250/-157	40	Break
	Base Metal ^(c)	-200/-129	90	Bend
		-225/-143	35	Break
	Electron Beam Welded ^(b)	-200/-129	91	Bend ^(d)
		-250/-157	35	Break
Ta-5W-1Re- 0.3Zr-0.025N (NASV-18)	TIG Welded ^(b)	+75/+24	96	Bend ^(d)
		-25/-32	20	Break
	Base Metal ^(b)	< -320/< -195	--	
		at -320/-195	91	Bend
	Electron Beam Welded ^(b)	< -320/< -195	--	
		at -320/-195	91	Bend
	TIG Welded ^(b)	< -100/< -73	--	
		at -100/-73	100	Bend

(a) Sheet annealed for 1 hr at 1650°C/3000°F prior to welding. Bend Radii - 1.8t

(b) Sheet processed from extruded ingot.

(c) Sheet processed from forged ingot.

(d) Sample exhibited ductile failure within weld and heat effected zone.

(e) Sample exhibited base metal failure.

determine the correlation between the DBTT and the interstitial, rhenium, total substitutional solute, and/or total tungsten equivalent contents (see Table 7). The total tungsten equivalent content (a/o) is derived from binary room temperature hardness data which show that for 1 a/o addition to tantalum, 1 a/o Re is 3 times more effective in increasing hardness than 1 a/o W, while Mo, Hf, and Zr are essentially the same as W. For the base metals, the DBTT's were consistently between -143°C (-225°F) and -115°C (-175°F), with the exception of that for NASV-18, which was less than -195°C (-320°F), most likely due to the alloy's lower solute content. As previously observed, EB welding had little or no effect on the DBTT of the base metals. The 56°C (100°F) increase in the case of NASV-16 is inconsistent with the other data. No correlation between the DBTT and any of the above mentioned compositional variations is apparent for either the base metal or for the EB welded material.

TIG welding appreciably increased the DBTT of all of the alloys. This data, plotted in Figures 1 and 2, show the dependence of the DBTT on the interstitial content and on the rhenium and total tungsten equivalent contents, respectively. The interstitial content is given in ppm of carbon plus nitrogen as actually analyzed, while the rhenium and total tungsten equivalent contents are given in nominal atom percent which is essentially identical to the analytical results (see Table 4). It appears that the interstitial content should be maintained below about 250 ppm in the presence of a high rhenium and/or high total tungsten equivalent content for good ductility in the as-welded condition. The DBTT of compositions with slightly higher interstitial contents could undoubtedly be improved with proper post weld heat treatments. It would also appear that for an interstitial content of about 250 to 300 ppm, (values given in brackets in Figure 2 are actual analyzed contents) rhenium should be maintained at something less than 1 weight percent. However, replotting the DBTT data versus total equivalent tungsten content (a/o) indicates that it is most likely this parameter rather than the rhenium content that effects the transition temperature. Thus for a 250 to 300 ppm interstitial content, the equivalent tungsten content should be maintained at something less than 10 a/o for satisfactory weldability. As indicated by the position of composition NASV-13 in both parts of Figure 2, the equivalent tungsten content can be increased appreciably as the interstitial content is decreased.

TABLE 7 - Summary of Ductile-Brittle Transition Temperature Data for Optimization Compositions^(a)

Composition and Heat No.	Condition	DBTT ^(f) °F/°C	Interstitial Content ^(b) (a/o)	Rhenium Content ^(c) (a/o)	TSSC ^(d) (a/o)	TWEC ^(e) (a/o)
Ta-7.5W-1.5Re -0.5Hf-0.015C -0.015N (NASV-12)	Base metal	-175/-115	270	1.5	9.5	12.5
	EB welded	-200/-129				
	TIG welded	0/-18				
Ta-6.5W-2.5Re -0.3Hf-0.01C -0.01N (NASV-13)	Base metal	-225/-143	195	2.5	9.3	14.3
	EB welded	-225/-143				
	TIG welded	-150/-101				
Ta-4W-1Mo-2Re -0.3Zr-0.015C -0.015N (NASV-14)	Base metal	-200/-129	270	2.0	8.6	12.5
	EB welded	-175/-115				
	TIG welded	+25/-4				
Ta-9.5W-0.5Re -0.25Zr-0.02C -0.01N (NASV-16)	Base metal	-200/-129	283	0.5	10.5	11.5
	EB welded	-100/-73				
	TIG welded	+75/+24				
Ta-4W-3Re-0.75Hf -0.01C-0.02N (NASV-17)	Base metal	-200/-129	270	3.0	7.75	13.75
	EB welded	-200/-129				
	TIG welded	+75/+24				
Ta-5W-1Re-0.3Zr -0.025N (NASV-18)	Base metal	<-320/-195	250	1.0	6.6	8.6
	EB welded	<-320/-195				
	TIG welded	<-100/-73				

(a) All sheet material annealed for 1 hr. at 1650°C/3000°F prior to welding and/or testing.

(b) Chemically analyzed carbon plus nitrogen in ppm.

(c) Nominal atom percent.

(d) Total substitutional solute content based on nominal atom percents.

(e) Total tungsten equivalent content based on nominal atom percents.

(f) Bend radius, 1.8t

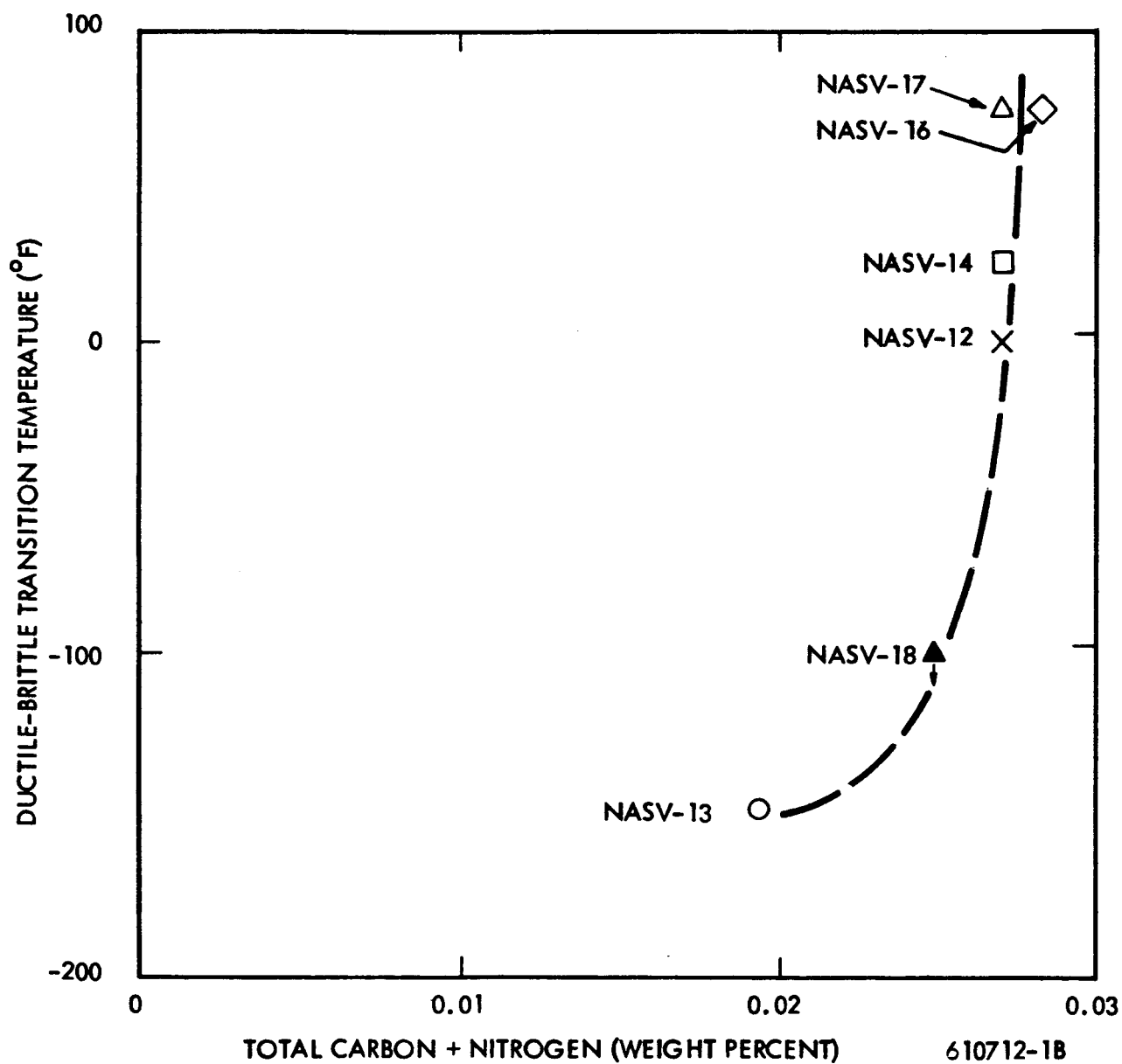


FIGURE 1 - Effect of Interstitial Content (Analyzed Content) on the Ductile-Brittle Transition Temperature of TIG Welded Optimization Compositions

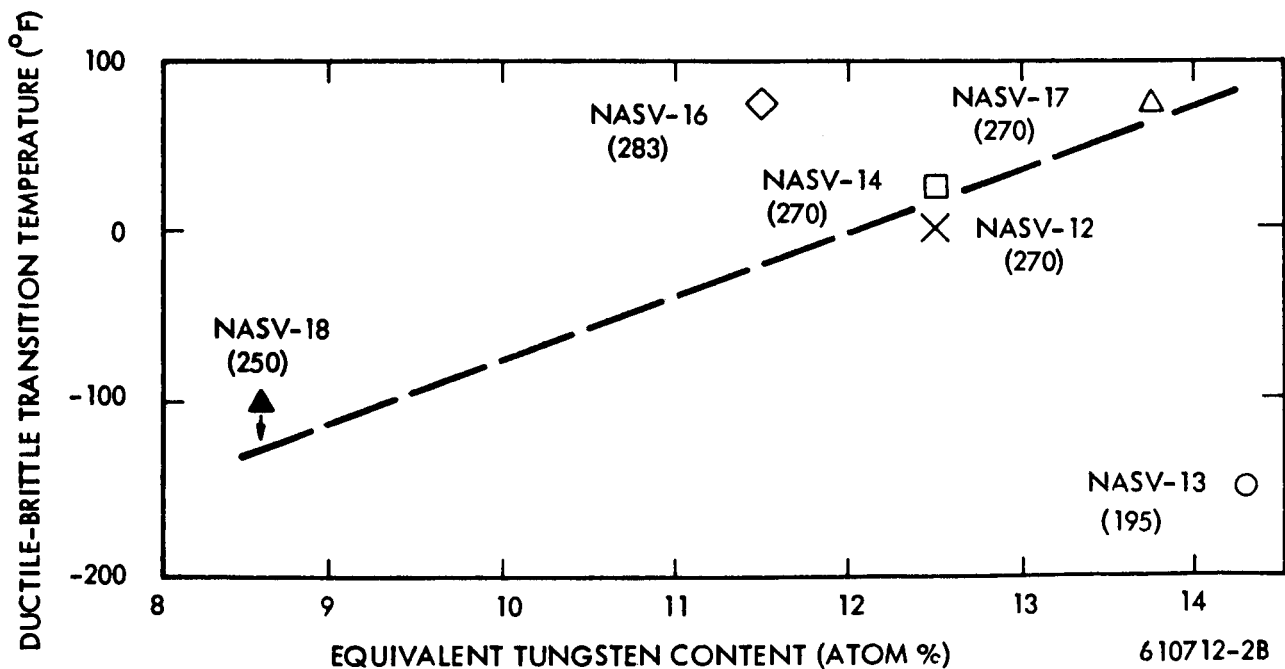
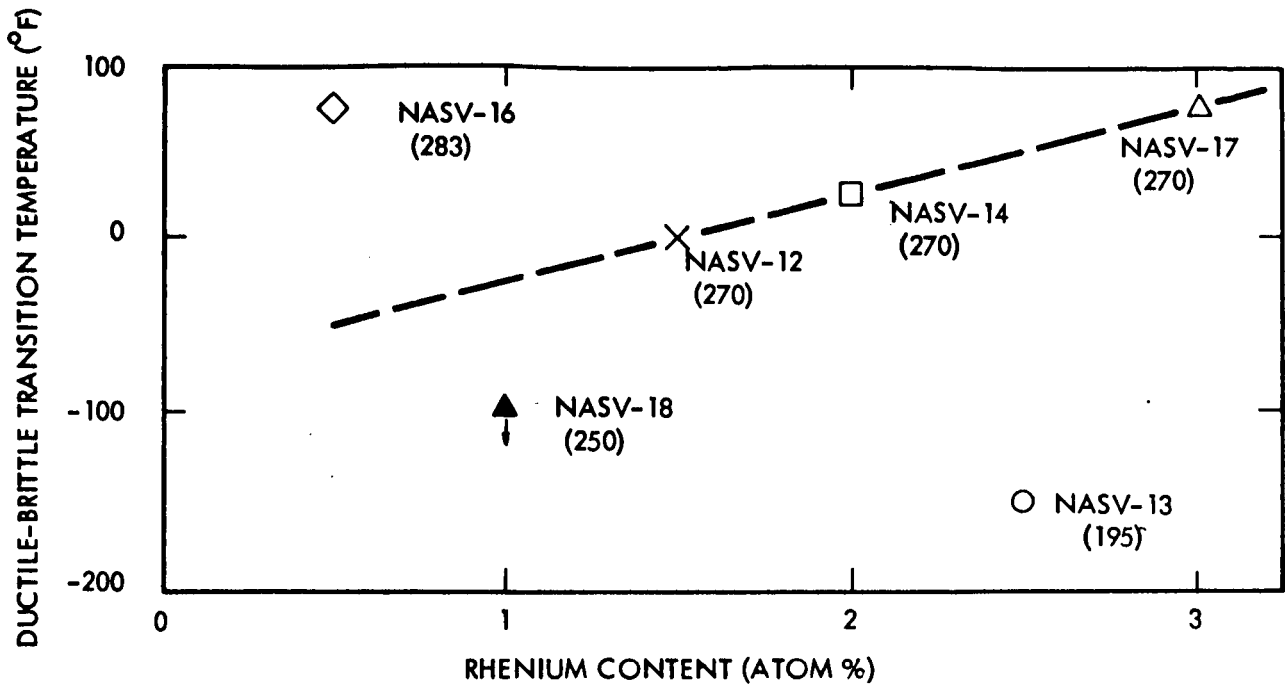


FIGURE 2 - Effect of Rhenium and Equivalent Tungsten Contents on the Ductile-Brittle Transition Temperature of As-TIG Welded Optimization Compositions Tested over Bend Radius of 1.8t. (Analyzed C + N values in parentheses)

As in the case of EB weld data, the results for the TIG welded sample of composition NASV-16 appear to be inconsistent with the results for TIG welded samples of the other optimization compositions. The expected DBTT for this sample, containing 0.5 percent rhenium and just slightly more than 250 ppm interstitials, was below -18°C (0°F). Furthermore, failure occurred in the base metal. As this behavior was unexpected, sections of extruded sheet bar of compositions NASV-16 and NASV-17 are being processed to sheet, which will be used to redetermine the DBTT's of the TIG welded samples and of the base metals.

Mechanical Property Evaluation

a. Tensile Properties - Tensile properties were obtained on compositions NASV-14, 16, 17, and 18. The data are reported in Table 8. Also included in Table 8, are previously reported data on compositions NASV-12, 13, and 14. With the exception of composition NASV-18, very minor differences existed in the tensile properties of these optimization compositions over the whole range of testing temperature. The lower tensile properties of composition NASV-18 are probably due to its lower substitutional solute content. All of the specimens were obtained from 0.040 inch sheet, processed from both upset forgings and extruded bar stock, and were annealed for 1 hour at 1650°C (3000°F) prior to testing.

b. Creep Properties - Creep data for the optimized compositions NASV-12, 13, 14, 16, 17, and 18 are reported in Table 9. These data* were plotted using the Larson-Miller parameter $(T+460)(20+\log t)$ where T is temperature in $^{\circ}\text{Fahrenheit}$ and t is the time for 1% strain in hours. The resultant curves are shown in Figure 3. Similar data obtained for T-111 and T-222 are also included on this plot. All the optimized compositions except NASV-18 exhibit significantly better creep properties under the conditions of test than do either T-111 or T-222. NASV-12 ($\text{Ta}-7.5\text{W}-1.5\text{Re}-0.5\text{Hf}-0.015\text{C}-0.015\text{N}$) exhibited the best creep resistance at both temperatures. NASV-12 is identical with NAS-36 ($\text{Ta}-5.7\text{W}-1.56\text{Re}-0.7\text{Mo}-0.25\text{Hf}-0.13\text{Zr}-0.015\text{C}-0.015\text{N}$) except the Mo and Zr were replaced with equivalent amounts of W and Hf respectively.

*Data obtained on 0.04-inch thick specimens annealed one hour at $1650^{\circ}\text{C}/3000^{\circ}\text{F}$ prior to test.

TABLE 8 - Mechanical Properties ^(a) of Compositions NASV-12 through NASV-18

Composition and Heat No. _(c)	Test Temperature (°F/°C)	0.2% Yield Strength (psi)	UTS (psi)	% Elongation		% Reduction in Area
				Uniform	Total	
Ta-7.5W-1.5Re -0.5Hf-0.015C -0.015N (NASV-12)	R. T./25	132,200	138,800	8.6	15.3	55.0
	2200/1205	38,100	56,500	--	25.3	--
	2400/1316	32,200	44,900	--	28.7	--
	2600/1427	31,300	37,500	--	36.0	--
	2800/1538	25,400	28,900	--	49.5	--
Ta-6.5W-2.5Re -0.3Hf-0.01C -0.01N (NASV-13)	R. T./25	142,000	146,300	6.5	12.7	57.5
	2200/1205	39,900	53,800	--	26.5	--
	2400/1316	32,300	42,800	--	31.2	--
	2600/1427	30,300	35,300	--	37.6	--
	2800/1538	22,900	26,000	--	42.5	--
Ta-4W-1Mo-2Re -0.3Zr-0.015C -0.015N (NASV-14)	R. T./25	138,200	142,700	10.4	17.3	55.1
	2200/1205	39,300	62,400	--	20.1	--
	2400/1316	37,000	51,500	--	27.9	--
	2600/1427	26,200	31,200	--	52.7	--
	2800/1538	23,000	25,400	--	30.7	--

TABLE 8 - Mechanical Properties of Compositions NASV-12 through NASV-18
(^a)
(Continued)

Composition and Heat No. (c)	Test Temperature (°F/°C)	0.2% Yield Strength (psi)	UTS (psi)	% Elongation		% Reduction in Area
				Uniform	Total	
Ta-9.5W-0.5Re -0.25Zr-0.02C -0.01N (NASV-16)	R. T./25	100,500	116,000	15.70	27.75	50.60
	R. T./25	102,000	116,400	15.85	28.85	49.30
	R. T./25	100,600	115,800	15.15	27.95	48.70
	2200/1205	38,900	62,100	--	20.6	--
	2400/1316	34,100	47,700	--	24.0	--
	2600/1427	31,700	39,000	--	29.4	--
	2800/1538	29,800	33,100	--	24.3	--
Ta-4W-3Re-0.75Hf -0.01C-0.02N (NASV-17)	R. T./25	132,000	133,600	12.25	24.50	55.60
	R. T./25	132,000	133,200	11.90	22.70	46.00
	R. T./25	130,600	131,000	13.10	25.30	45.60
	2200/1205	39,400	56,300	--	21.8	--
	2400/1316	34,800	45,600	--	28.8	--
	2600/1427	33,700	38,200	--	40.5	--
	2800/1538	25,400	27,600	--	50.4	--

TABLE 8 - Mechanical Properties ^(a) of Compositions NASV-12 through NASV-18
(Continued)

Composition and Heat No. ^(c)	Test Temperature (°F/°C)	0.2% Yield Strength (psi)	UTS (psi)	% Elongation		% Reduction in Area
				Uniform	Total	
Ta-5W-1Re-0.3Zr -0.025N (NASV-18)	R. T./25	110,300	112,300	11.65	18.50	42.70
	2200/1205	29,300	46,400	--	21.2	--
	2400/1316	25,700	39,700	--	25.8	--
	2600/1427	21,400	28,600	--	40.3	--
	2800/1538	20,800	22,700	--	45.8	--
	R. T./25 ^(b)	105,700	113,500	13.15	19.55	54.20

(a) Strain rate 0.05 in/in/min throughout test.

(b) Strain rate 0.005 in/in/min through 0.6% yield and then 0.05 in/in/min for balance of test.

(c) All material annealed one hour at 1650°C (3000°F) prior to test.

TABLE 9 - Creep Properties^(e) of Optimized Tantalum Alloys at 1×10^{-8} Torr

Composition	Test Temperature (°C/°F)	Applied Stress (psi)	Test Time (hrs)	Total Elongation (%)	Time to 1% Elong. (hrs)	Room Temp. Hardness	
						Pre-Test (DPH)	Post-Test (DPH)
NASV-12 Ta-7.5W-1.5Re-0.5Hf -0.015C-0.015N							
NASV-12-B-1C ^(a)	1315/2400	15,000	210.2	0.01	--	--	--
NASV-12-B-1C ^(c)	1315/2400	15,000	444.6	0.39	(1,140) ^b	--	268
NASV-12-B-2C ^(d)	1315/2400	12,680	257.8	-0.09	--	--	--
NASV-12-B-2C ^(d)	1315/2400	20,180	171.1	7.93	54	--	269
NASV-12-E-3C ^(d)	1427/2600	8,000	512.9	0.89	(575)	--	277
NASV-12-E-3C ^(d)	1427/2600	10,000	260.5	6.47	78	277	283
NASV-12-E-4C	1427/2600	12,790	188.0	9.60	68	308	277
NASV-13 Ta-6.5W-2.5Re-0.3Hf -0.01C-0.01N							
NASV-13-B-1C	1315/2400	15,000	212.4	0.31	(685)	--	--
NASV-13-B-2C	1315/2400	12,620	284.0	0.21	(1,350)	--	--
NASV-13-E-3C	1427/2600	8,000	194.0	0.62	312	312	265
NASV-13-E-4C	1427/2600	10,000	330.0	2.54	153	301	257
NASV-14 Ta-4W-1Mo-2Re-0.3Zr -0.015C-0.015N							
NASV-14-B-1C	1315/2400	15,000	230.3	0.41	(562)	--	246
NASV-14-B-2C	1315/2400	12,810	211.1	0.12	(1,750)	--	249
NASV-14-E-3C	1427/2600	7,950	187.1	0.79	(237)	299	293
NASV-14-E-4C	1427/2600	10,000	260.0	2.20	171	291	--

TABLE 9 - Creep Properties (e) of Optimized Tantalum Alloys at 1×10^{-8} Torr (Continued)

Composition	Room Temp. Hardness					
	Test Temperature (°C/°F)	Applied Stress (psi)	Test Time (hrs)	Total Elongation (%)	Time to 1% Elong. (hrs)	Post-Test (DPH)
NASV-16 Ta-9.5W-0.5Re-0.25Zr -0.02C-0.01N						
	1315/2400	15,000	195.9	0.40	(490)	284
	1315/2400	12,500	234.9	0.16	(1,470)	281
	1427/2600	8,000	208.6	0.56	(370)	285
	1427/2600	10,000	285.5	2.60	150	280
NASV-17 Ta-4W-3Re-0.75Hf -0.01C-0.02N						
	1315/2400	15,000	200.0	0.29	(690)	323
	1315/2400	12,500	283.8	0.27	(1,050)	322
	1427/2600	10,000	210.5	1.46	175	322
	1427/2600	8,000	331.2	0.96	(346)	323
NASV-18 Ta-5W-1Re-0.3Zr-0.025N						
	1315/2400	15,000	93.0	2.10	67	277
	1427/2600	10,000	117.0	6.58	42	279
NASV-18-B-1C						--
NASV-18-E-3C						224

- Identification denotes whether specimen from sheet processed from -B- upset forging or -E- dynapak extrusion.
- Values enclosed with parentheses were estimated by extrapolation.
- Test unloaded, measured at room temperature, then re-inserted and the test continued for a total of 444.6 hours at 15,000 psi and 2400°F.
- Test reloaded at higher stress level for time indicated.
- All specimens were annealed for 1 hr. at 1650°C (3000°F) prior to creep testing.

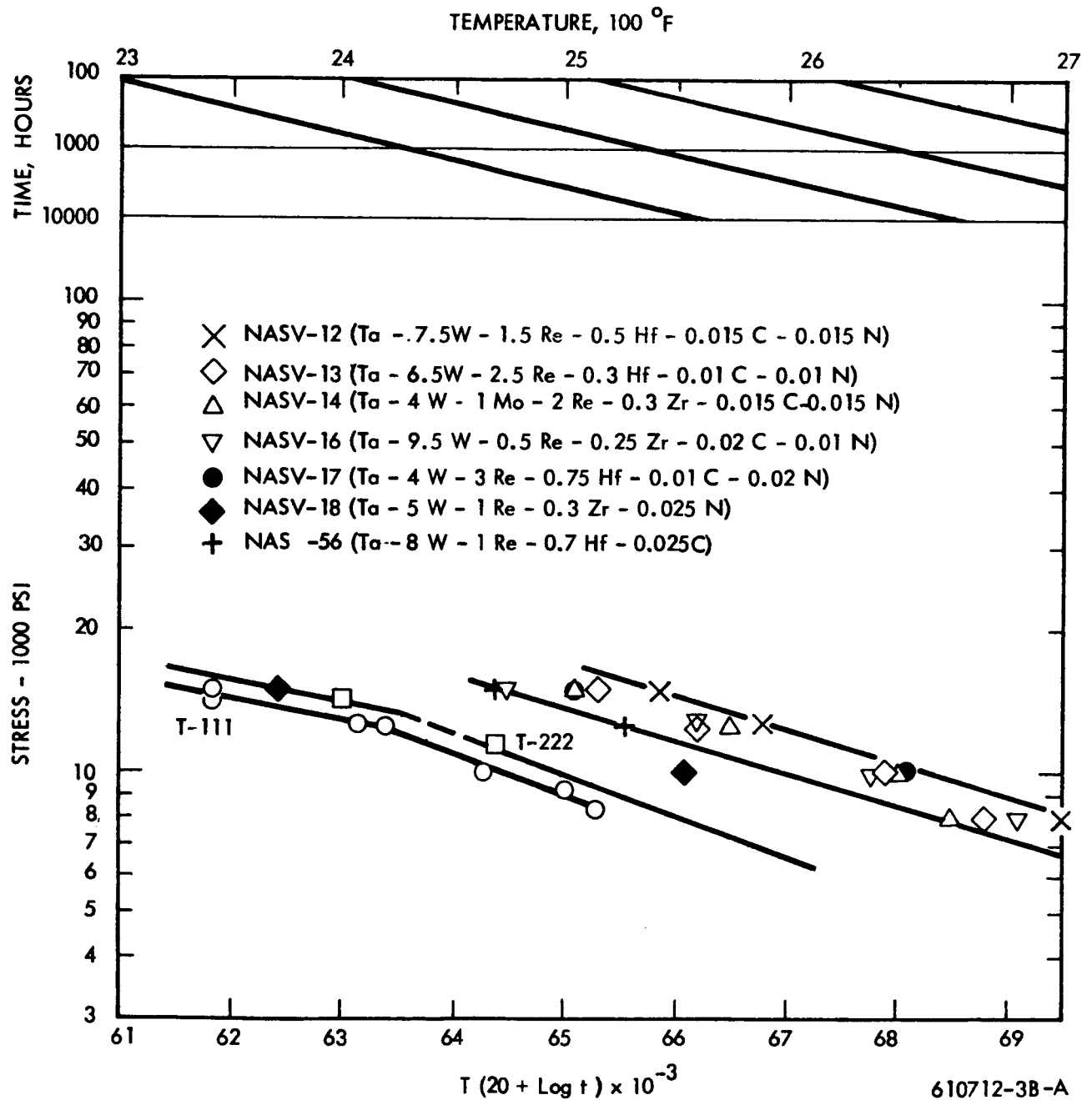


FIGURE 3 - Creep Properties of the Optimization Compositions Based on the Larson-Miller Parameter (where t = time to 1% strain in hours (all material annealed for one hour at 1650°C(3000°F) prior to test).

Creep properties of NASV-18 are equivalent to T-222 at 2400°F and 15,000 psi but slightly better at 2600°F and 10,000 psi. This is of particular significance since NASV-18 contains only 6.6 a/o substitutional solute versus the 12-14% normally found in T-222. Nitrogen was the intentional interstitial addition to NASV-18. It has been shown previously³ that nitrogen interacts with Hf and Zr to form a coherent precipitate with the tantalum alloy matrix after a specified solution annealing treatment followed by a low temperature aging treatment. Although overaging of the ZrN occurs at 1315°C (2400°F) at times in excess of 1 hour, the creep resistance of overaged alloys still showed significant improvement over T-222 under similar conditions of test. However, much more study is required to inter-relate the degree of nitrogen supersaturation with precipitation kinetics and the resulting effects on strength and fabricability. The response of the nitrogen bearing alloys to heat treatment make this system one worthy of extensive investigation.

The role of the substitutional and interstitial additions on the creep resistance of Ta is complex as is evident from the data plotted in Figures 4, 5, and 6. The time to 1% strain is the property used as the criteria for creep resistance.

Looking first at the effect of total substitutional solute addition (see Figure 4) it is evident that a poor correlation exists. Neglecting the interstitial content of 200-300 ppm, it would appear that the creep behavior is strongly affected not so much by the amount of substitutional solute but apparently by the species. A re-plotting of the data at 2400°F and 2600°F as a function of total W a/o equivalent (Figure 5) indicates that increasing the substitutional solute addition improves creep resistance. This would be expected when the solute has a significantly higher elastic modulus than the solvent.⁴ The addition of significant amounts of Hf have been shown to degrade creep properties at 2400°F and this is probably why the data for T-111 and T-222 do not fit the curves in Figure 5. However from a liquid alkali metal corrosion consideration, the presence of some reactive element (Hf or Zr) is essential.

From the data plotted in Figure 6 it appears that interstitials (presumed to have reacted with the reactive metal addition to form carbides and/or nitrides) significantly

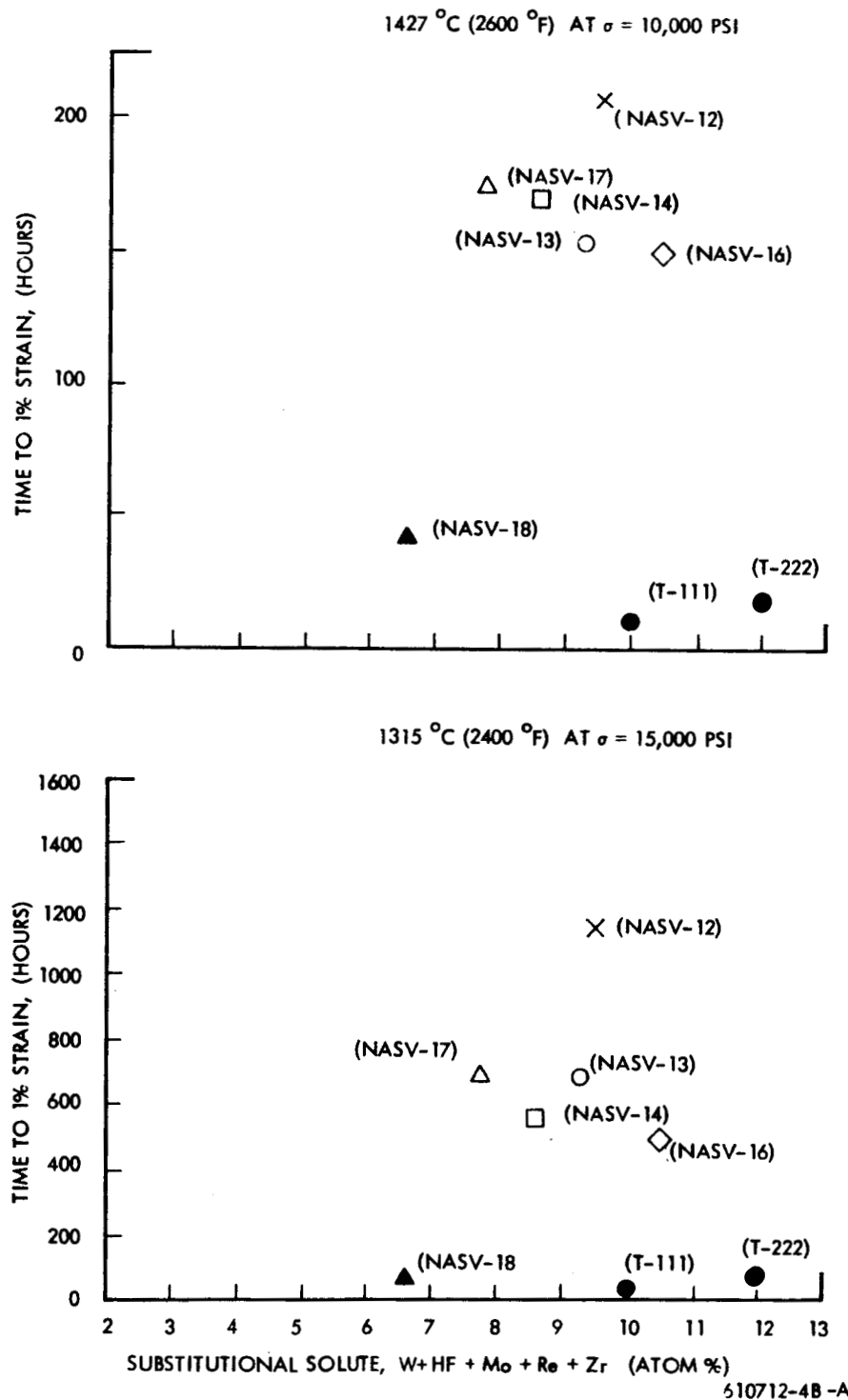
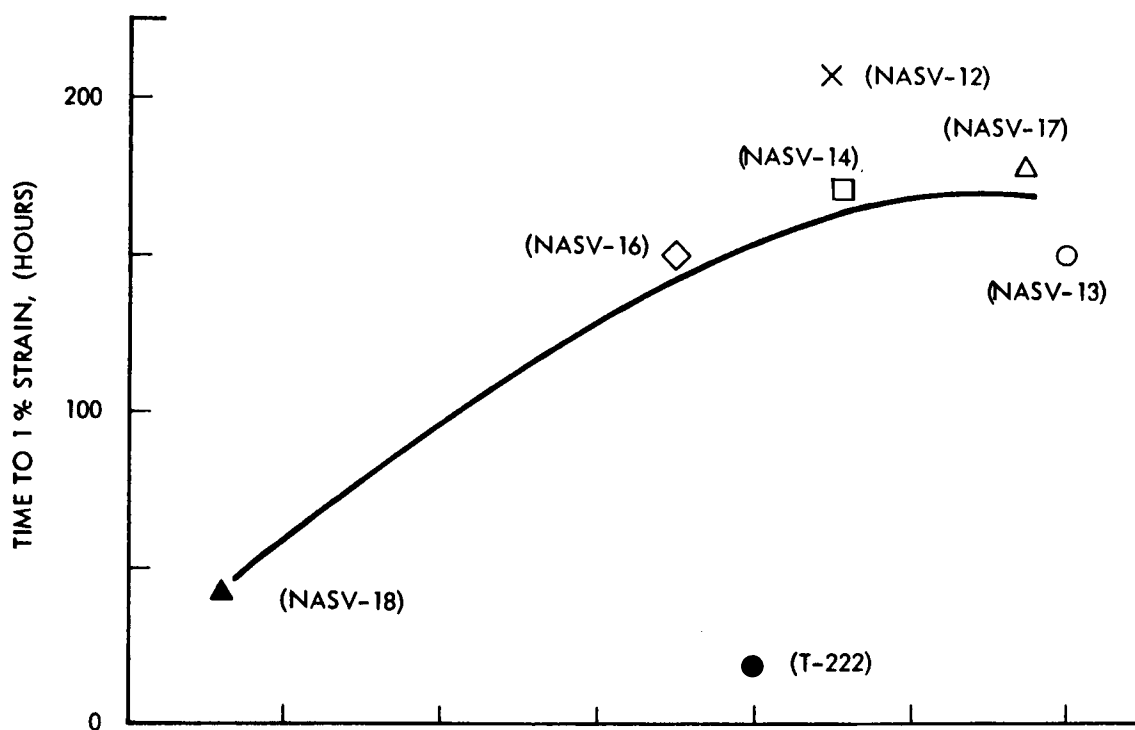


FIGURE 4 - Effect of Substitutional Solute Content on the Creep Behavior of the Optimization Compositions (Note: Specimens annealed one hour at 1650 °C (3000 °F) prior to test).

1427 °C (2600 °F) AT $\sigma = 10,000$ PSI



1315 °C (2400 °F) AT $\sigma = 15,000$ PSI

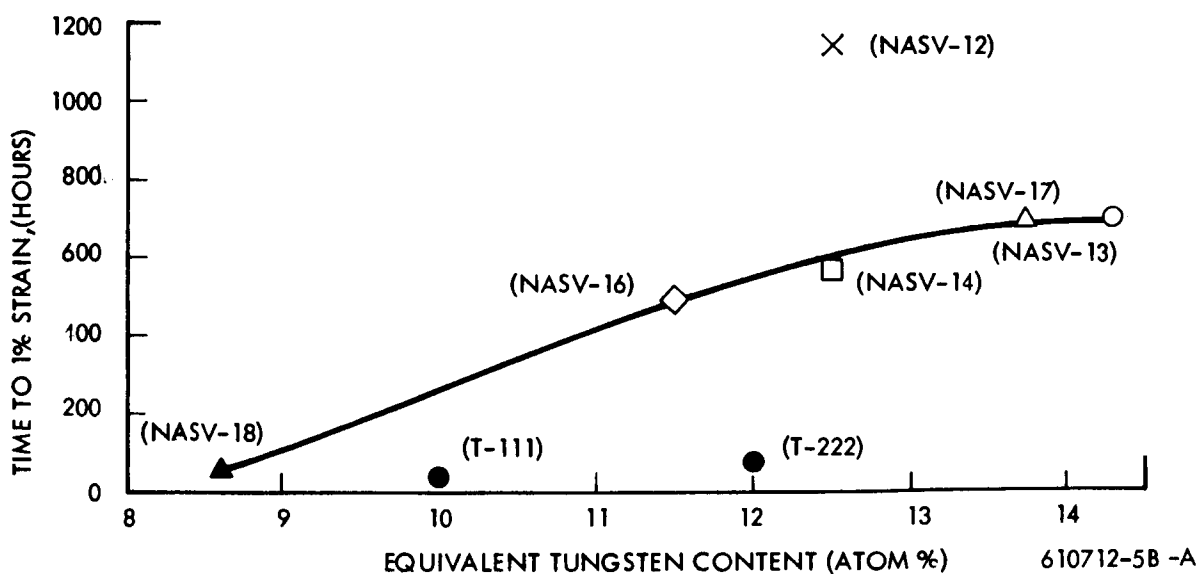
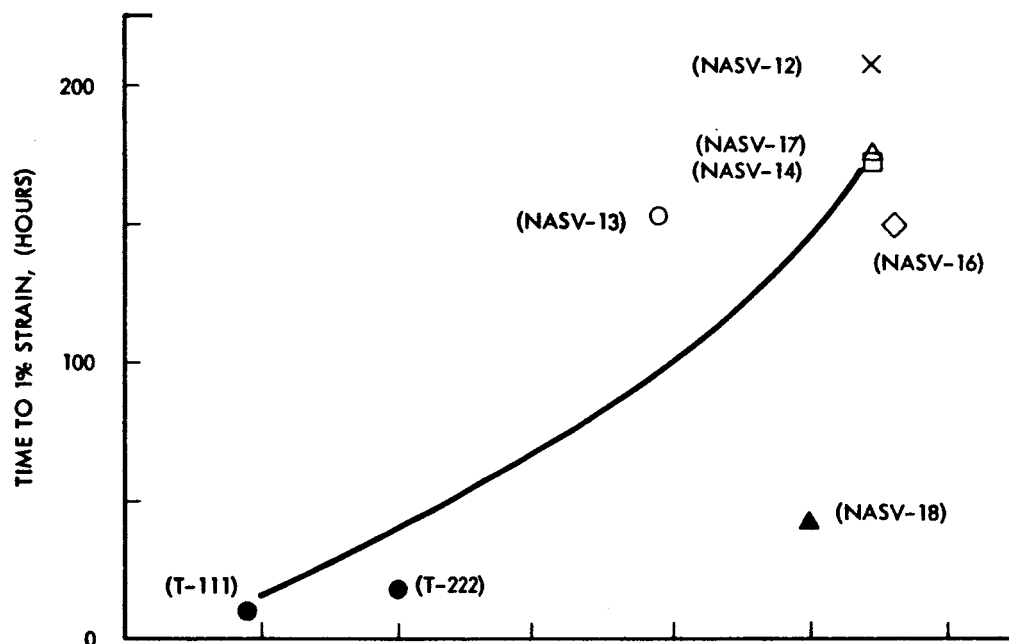


FIGURE 5 - Effect of Equivalent Tungsten Content* on the Creep Behavior of the Optimization Compositions. (*Equivalent Tungsten Content = %W + % Mo + % Zr + % Hf + 3 x % Re (Specimens annealed for one hour at 1650 °C (3000 °F) prior to test).

1427 °C (2600 °F) AT $\sigma = 10,000$ PSI



1315 °C (2400 °F) AT $\sigma = 15,000$ PSI

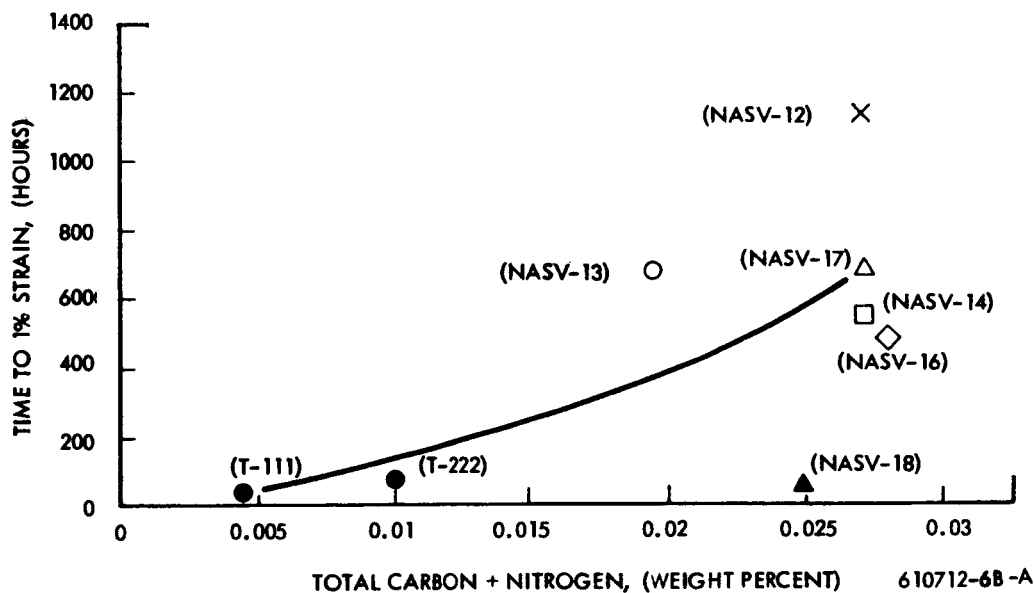


FIGURE 6 - Effect of Interstitial Content on the Creep Behavior of the Optimization Compositions (Specimens annealed for one hour at 1650°C (3000°F) prior to test).

effect creep resistance at 2400°F and 2600°F. However the effects of the interstitial/reactive metal interaction on creep behavior are complex and not well understood. From the room temperature hardness measurements taken before and after testing, it is evident that the observed softening is due to the precipitation of non-coherent carbides and nitrides. The kinetics of the precipitation reaction are accelerated by the applied stress. Retesting at a higher stress level of a specimen previously tested results in a poorer creep resistance than would be expected if the test were started with the specimen in the solution annealed condition. For example, at 2600°F, NASV-12, tested at 12,790 psi and 8,000 psi elongated 1% in 68 and 575 hours respectively. Thus using a Larson-Miller interpolation of this data, NASV-12 under an applied stress of 10,000 psi at 2600°F would require 208 hours to elongate 1%. However on reloading to 10,000 psi, the specimen tested previously at 8,000 psi elongated 1% in only 78 hours.

Rhenium appears to have the most significant effect on creep resistance, the greatest change occurring between 0% Re and 1/2% Re. The data plotted in Figure 7 indicate that a very small rhenium addition (~0.5 a/o) has a very pronounced effect on the creep behavior resulting in a 5X increase at 2400°F and 10X at 2600°F. Increasing the rhenium from 0.5 to 3 a/o, a six fold increase, however only resulted in an 18% increase in time to reach 1% strain at 2600°F and 10,000 psi and a 38% increase at 2400°F and 15,000 psi.

B. FOUR INCH DIAMETER INGOT SCALE-UP

Processing of the NASV-20 composition (Ta-8W-1Re-0.7Hf-0.025C) continued. This alloy was selected as a rhenium containing carbide dispersion strengthened sheet and tubing alloy.

Primary Breakdown - A 1 inch long by 4 inch diameter section from the bottom end of the conditioned NASV-20 ingot was dip coated with the Al-12Si alloy and upset forged at 1400°C (2550°F) by a single blow of the Dynapak. Forging data are reported in Table 10, and the resulting high quality, 0.385 inch thick upset forging is shown in Figure 8. The average diamond pyramid hardness (for a 30 Kg load) of the forging was 338 compared to 237 for the as-cast material.

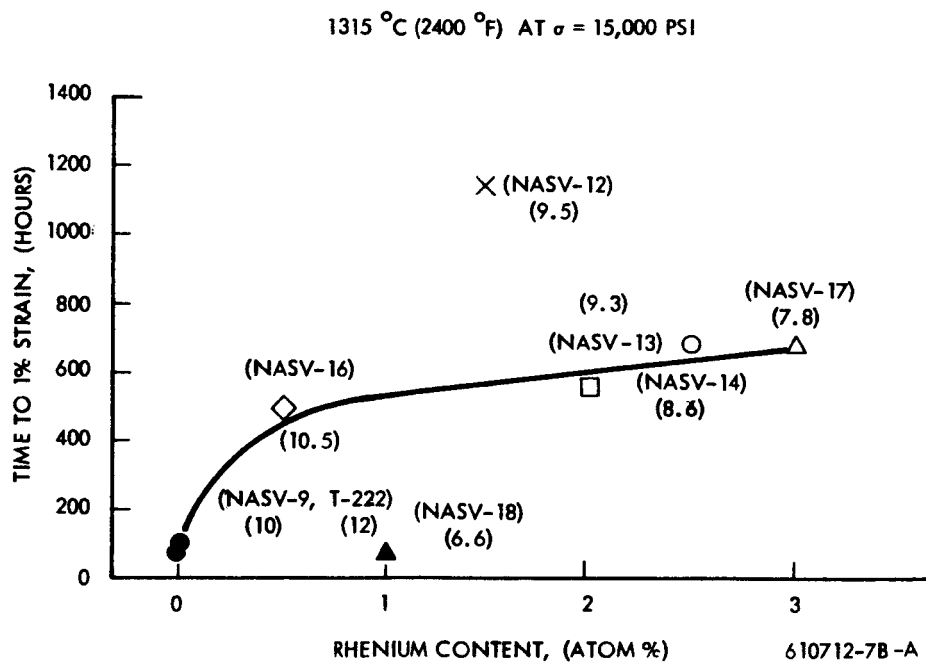
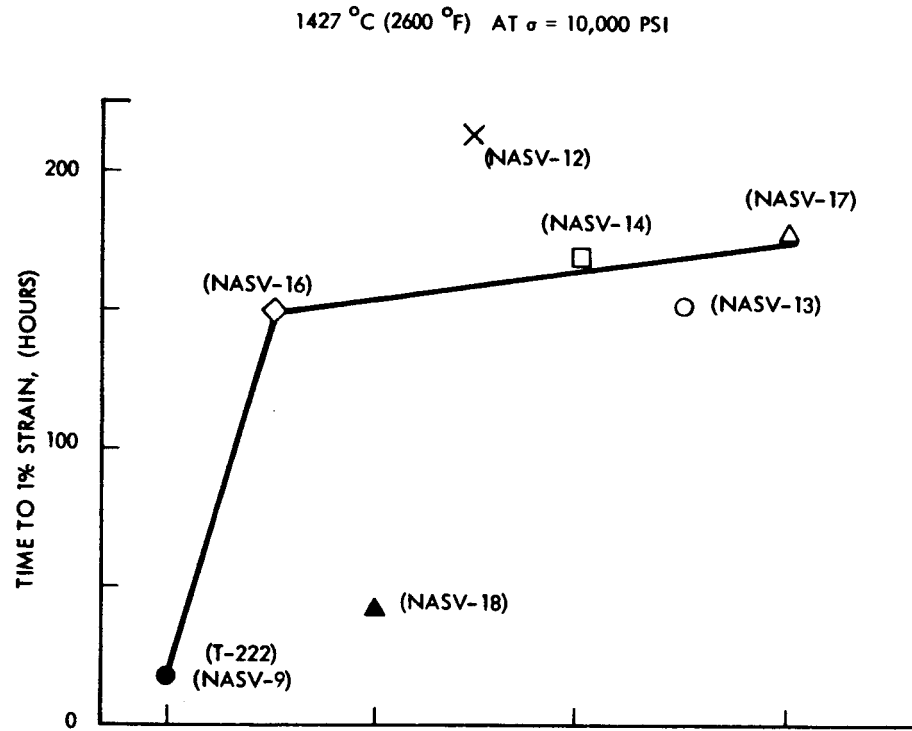


FIGURE 7 - Effect of Rhenium Content on the Creep Behavior of the Optimization Compositions (Specimens annealed for one hour at 1650°C (3000°F) prior to test).

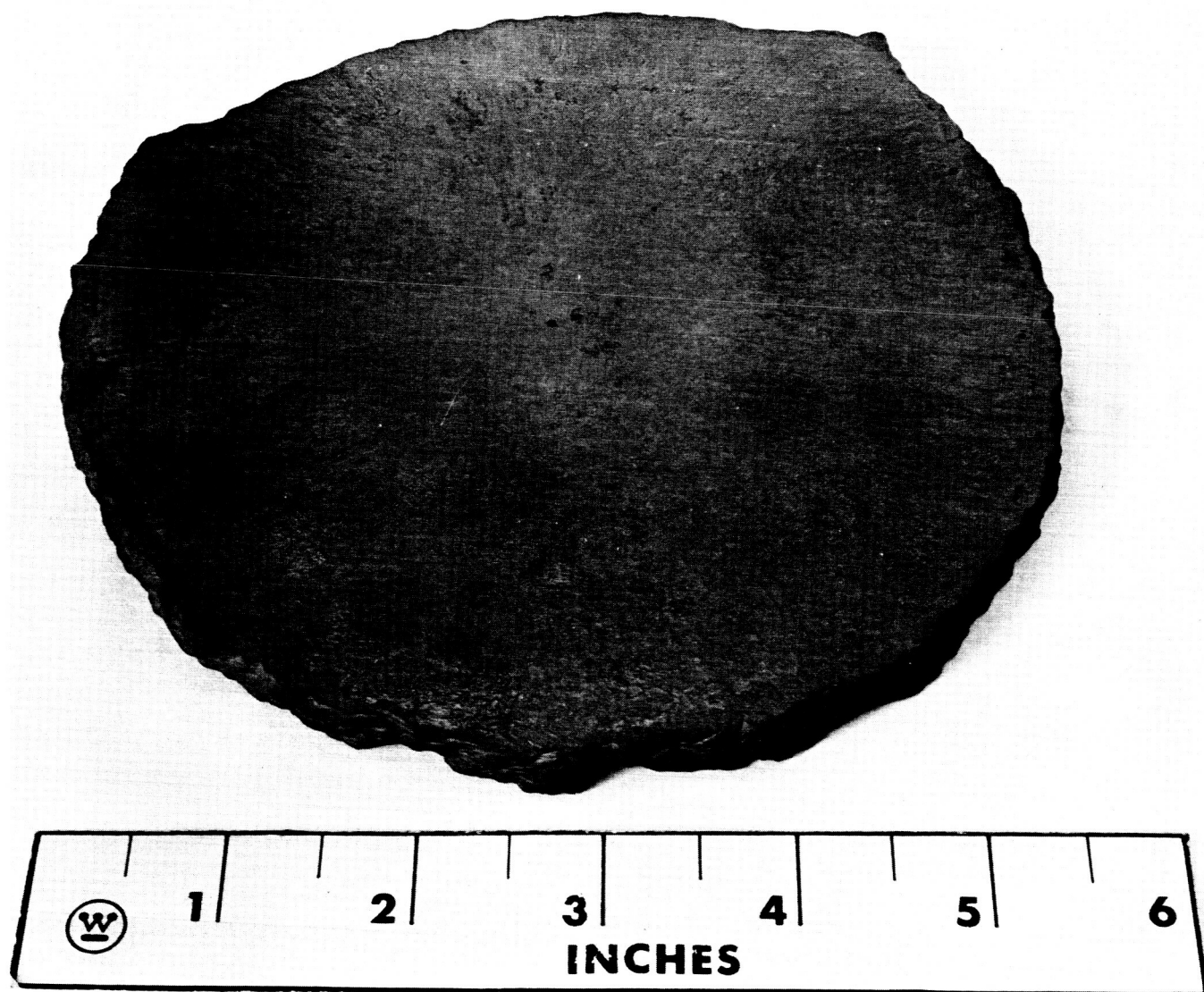


FIGURE 8 - Upset Forged Ingot of NASV-20 (Ta-8W-1Re-0.7Hf-0.025C)

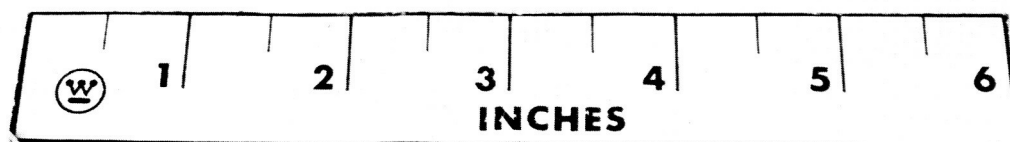
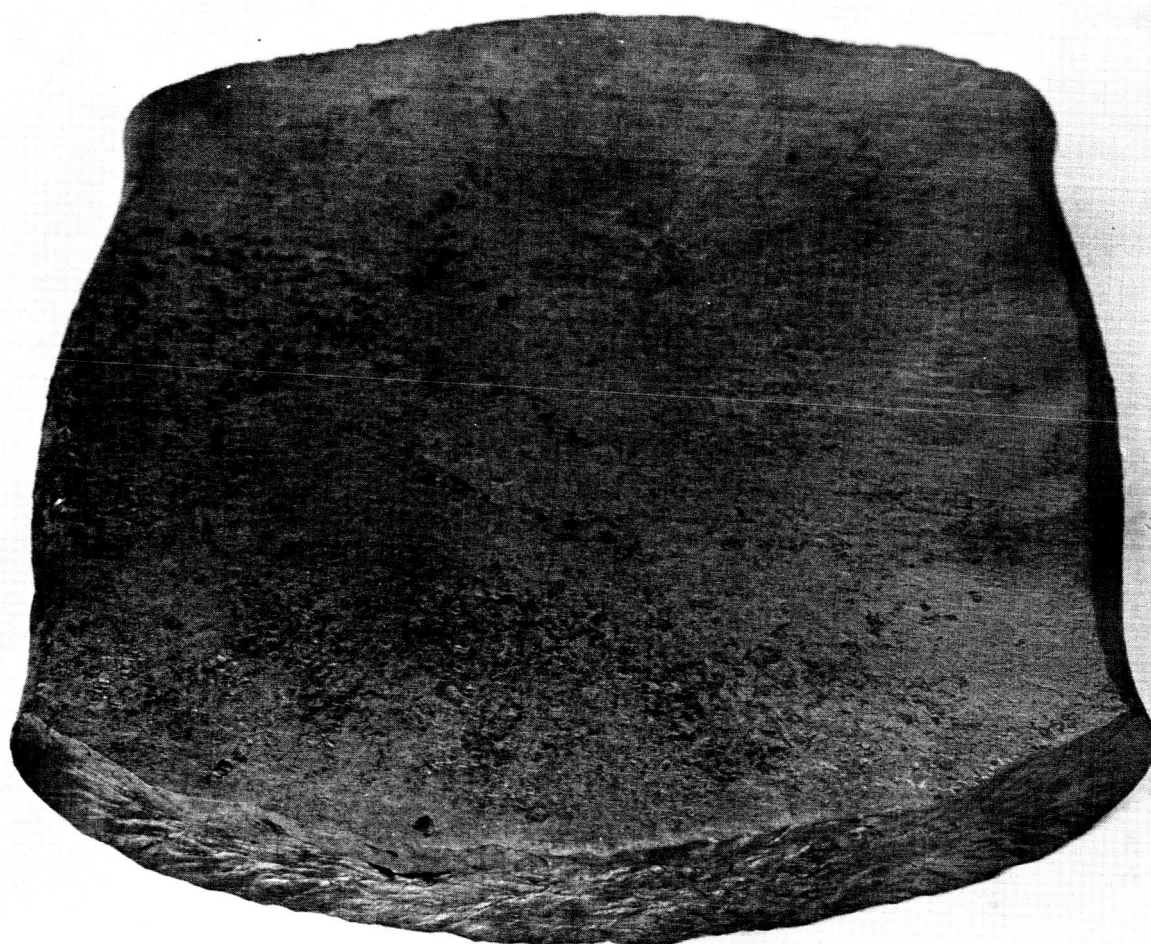


FIGURE 9 - Side Forged Ingot of NASV-20 (Ta-8W-1Re-0.7Hf-0.025C)

be rolled to 0.250 inch thickness at a maximum temperature of 500°C (930°F).

Chemical Analysis - Chemical analysis results, obtained on the as-cast NASV-20 ingot are reported in Table 11. Tungsten was present in a lesser amount than desired and hafnium appears to have been present in excess at the bottom end of the ingot. Carbon was uniformly distributed throughout the ingot at a level within 10 to 20 ppm of the nominal composition.

TABLE 11 - Chemical Analysis of Composition NASV-20
(Ta-8W-1Re-0.7Hf-0.025C)

Type and Position of Sample	Analysis (Weight Percent)					
	W	Re	Hf	C	N	O
Chips (Top)	7.4	1.04	0.71	0.024	0.0013	--
Chips (Bottom)	7.2	0.92	1.01	0.023	0.0027	--
Drillings (Bottom)	--	--	1.09	0.024	--	--
Chunks (Top)	--	--	--	--	--	0.0006
Chunks (Bottom)	--	--	--	--	--	0.0021

Weldability - EB and TIG bead-on-plate welds were made on 0.040 inch NASV-20 sheet, which had been annealed for 1 hour at 1650°C (3000°F) prior to welding. The DBTT's of these welded samples and of the NASV-20 base metal were determined. Table 12, which summarizes the data, illustrates the excellent weldability of this composition. The DBTT's are lower than expected from data previously obtained on compositions NAS-56⁵ (a non-consumable arc melted button having the same composition as NASV-20 and NASV-9^{1,5} (Ta-9W-1Hf-0.025C). As in the past EB welding had little or no effect on the DBTT of the

base metal, while TIG welding caused it to increase appreciably. Even so, the DBTT of the TIG welded material is greatly below the value predicted on the basis of either the rhenium or total tungsten equivalent content (see Figure 2, Page).

TABLE 12 - Ductile-Brittle Transition Temperatures of Composition NASV-20^a
(Ta-8W-1Re-0.7Hf-0.025C)

Condition	Temperature °F/°C	No Load Bend Angle (Degrees)	Remarks
Base Metal ^b	<-320/<-195 at -320/-195	96	No Failure
Electron Beam Welded ^b	<-320/<-195 at -320/-195	96	No Failure
TIG Welded ^c	(-175 to -250°F) (-115 to -157°C)	--	--

- a. Sheet material annealed for 1 hr. at 1650°C/3000°F prior to welding and/or testing.
- b. 0.040 inch sheet and 1.8t bend radii used.
- c. 0.035 inch sheet and 1t bend radii used.

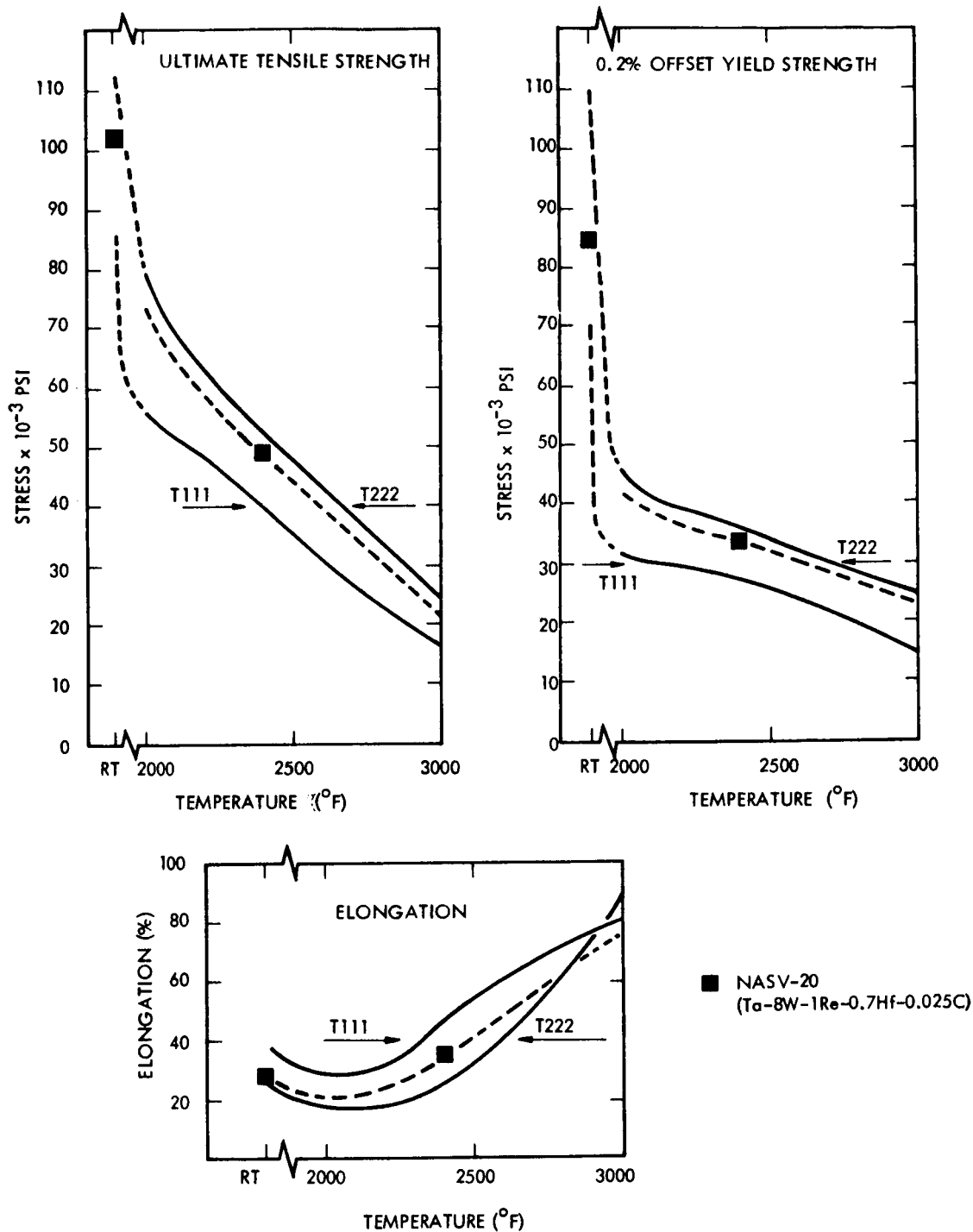
Mechanical Property Evaluation - Tensile data were obtained on three specimens of composition NASV-20, which had been machined from 0.040 inch sheet processed from the upset forging. Prior to testing, each specimen was annealed for 1 hour at 1650°C (3000°F). The results are recorded in Table 13. Over the temperature range of room temperature to about 1650°C (3000°F), the yield strength, ultimate tensile strength, and tensile elongation of NASV-20 are all intermediate to those of T-111 and T-222 (see Figure 10), while they are essentially identical to those of NASV-9.

Creep Properties - Although the short time properties of NASV-20 were essentially identical to those of NASV-9, the potent effect of the 1% Re addition is readily apparent on

**TABLE 13 - Mechanical Properties of Composition NASV-20^a
(Ta-8W-1Re-0.7Hf-0.025C)**

Test Temperature	0.2% Yield Strength (psi)	Ultimate Tensile Strength (psi)	% Elongation		% Reduction in Area
			Uniform	Total	
R. T. ^b	85,300	103,500	15.5	26.6	48.40
R. T. ^c	82,800	104,600	16.35	27.55	49.30
2400 ^d	30,400	40,900		35.0	

- a. Material processed from upset forging.
- b. Strain rate 0.05 in/in/min. throughout test.
- c. Strain rate 0.005 in/in/min. through 0.6% yield and then 0.05 in/in/min. for balance of test.
- d. Annealed one hour at 1650°C (3000°F) prior to test.



610712-8B-A

FIGURE 10 - Mechanical Behavior of NASV-20 (Ta-8W-1Re-0.7Hf-0.025C) as a Function of Temperature. (Specimens Annealed for 1 Hr. at 1650° C/ 3000° F Prior to Test).

the 2400°F creep properties. The data shown in Figure 11 are based on the Larson-Miller parameter and were obtained on sheet specimens processed from an 800 gram non-consumable melted button ingot.¹ Creep specimens have been machined from the sheet processed from the 4 inch diameter consumable electrode melted and testing will be initiated during the next report period.

Phase Identification and Morphology - As stated in the last quarterly report,² a detailed phase identification and morphology study will be conducted on the 4 inch diameter optimized compositions. During this period, this work was initiated on composition NASV-20, in the as-cast condition. The dispersed phases were extracted by dissolving the matrix in a bromine-methanol-tartaric acid solution^{2,6} and the extracted residue was analyzed by the standard Debye-Scherrer x-ray diffraction technique. Besides some undissolved BCC tantalum, only one phase was detected. This phase was the HCP dimetal carbide of tantalum, having lattice parameters, a_o and c_o , of 3.10 Å and 4.92 Å respectively, compared with values of 3.106 Å and 4.945 Å reported for Ta₂C.^{7,8} An x-ray fluorescence analysis of the residue indicated that its metallic composition was approximately 95% Ta and 5% W. No Hf was observed. As the fluorescence data precludes appreciable substitution of W and especially Hf for the Ta in the dimetal carbide, the reduction of the lattice parameters is apparently due to a carbon deficiency. Thus, the dimetal carbide phase can be accurately represented as (Ta,W)₂C_{1-x} rather than as (Ta,W,Hf)₂C_{1-x} as previously thought. The lattice parameter, a_o , of the BCC tantalum matrix was 3.29 Å, compared with the accepted value for unalloyed Ta of 3.3058 Å.* This reduction in the matrix lattice parameter size is due to the presence of W.

Figure 12 illustrates the microstructure of the as-cast material at 150, 500, and 1500X. The dimetal carbide is present in the form of platelets visible at 150X and as a fine dispersoid visible at 1500X.

Electron microscopy techniques, described in the last quarterly report² are presently being employed to better study the as-cast structure.

*ASTM card No. 4-0788 for Ta.

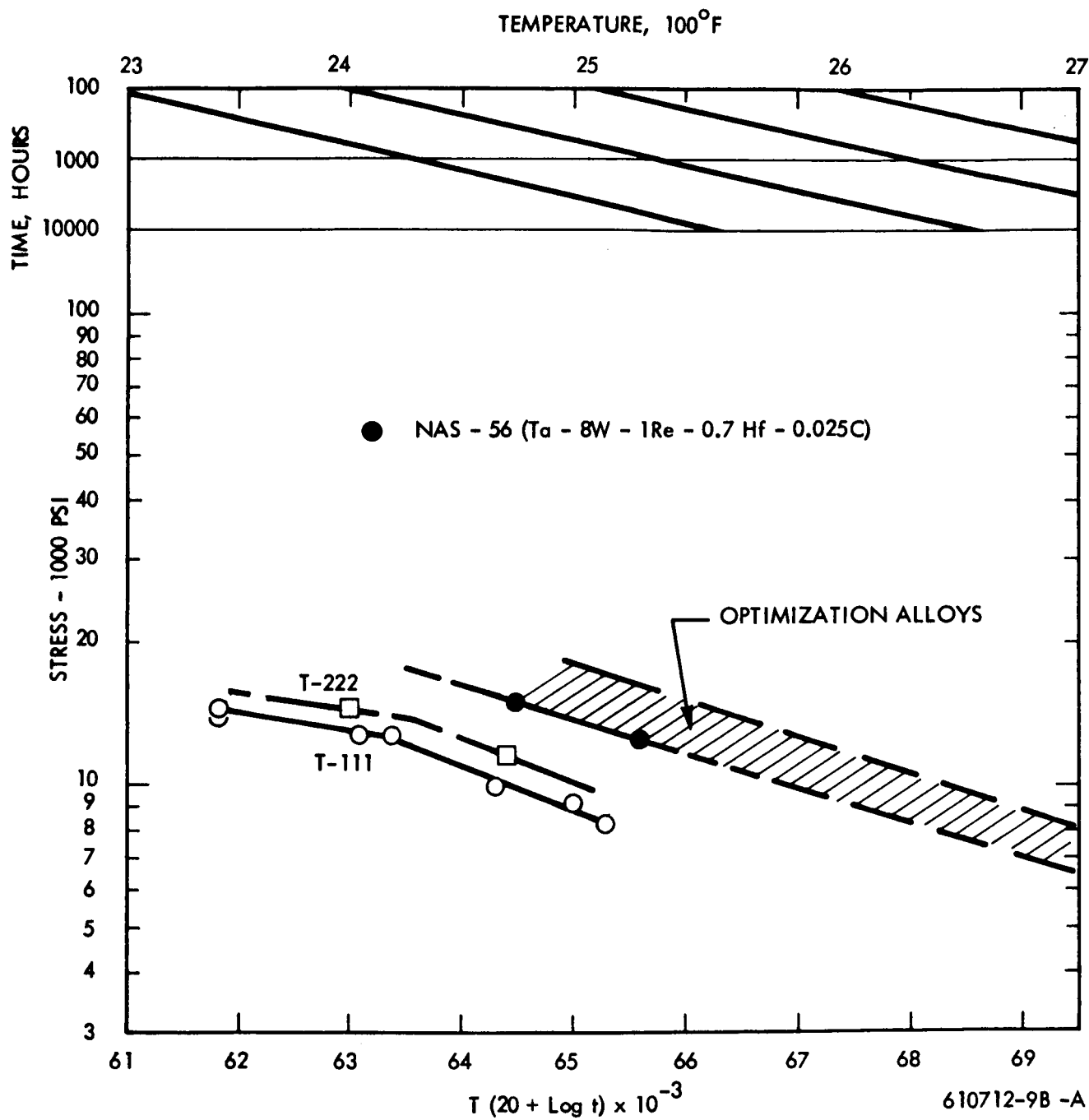
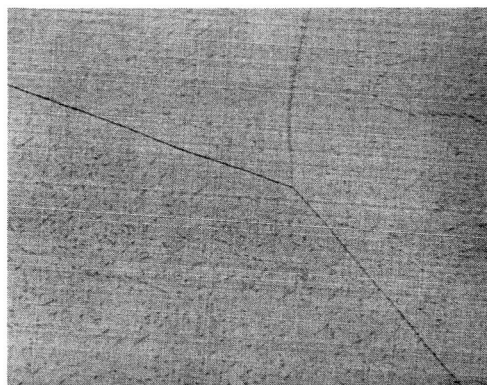


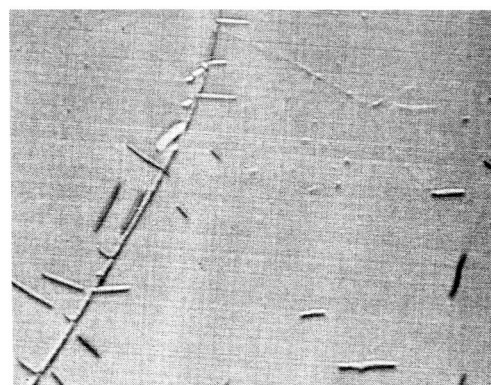
FIGURE 11 - Creep Properties of Fabricable Tantalum Base Alloys Based on the Larson-Miller Parameter, t = time to 1% strain (specimens annealed one hour at 1650°C (3000°F) prior to test.



a. 150X



b. 500X



c. 1500X

FIGURE 12 - Microstructure of As-Cast NASV-20 (Ta-8W-1Re-0.7Hf-0.025C) Showing Tantalum Dimetal Carbide Precipitate - Etchant (25% HNO_3 -25% HF-50% Glycerine)

C. TURBINE COMPOSITIONS

Secondary Processing - The conditioned 1 inch diameter extruded rod of composition NASV-15 (Ta-9W-1.5Re-1Hf-0.03N) was heat treated for 2 hours at 2000°C (3630°F) plus 2 hours at 1400°C (2550°F), and dip coated with an Al-12Si alloy. It was then swaged to a diameter of 0.425 inch at 1200°C (2190°F). The resulting high quality rod was centerless ground to 0.380 inch diameter and test specimens were machined from it. Hardness data for the various stages of processing are included in Table 14.

Chemistry - Chemical analyses results on composition NASV-15 are reported in Table 15. As with the optimization compositions, the ingot chemical analyses, with the exception of nitrogen, agree very well with the desired composition. The deficiency of nitrogen, ranging from 50 to 60 percent, was much greater than that encountered in the optimization compositions. The reason for the deficiency is not known, but the nitrogen is assumed to have been lost during melting.

Mechanical Properties - Room temperature tensile data were obtained on a second specimen of composition NASV-11 (Ta-9W-1.5Re-1Hf-0.015C-0.015N), in order to verify the anomalous tensile behavior of this material reported in the last quarterly report.² Again, the 0.2% offset yield strength was higher than the ultimate tensile strength. Furthermore, there was approximately a 13,000 psi difference between the upper and lower yield strengths. Data for both samples, which were similarly annealed for 1 hour at 1650°C (3000°F) prior to testing, are reported in Table 16. The observed yield point phenomenon could be explained by Cottrell's "theory of the sharp yield point"⁹ (i. e., the drop in the yield strength is associated with the increased mobility of dislocations after they have been freed from atmospheres of interstitial atoms which previously immobilized them). The absence of appreciable strain hardening of the alloy precluded its ultimate tensile strength from equalling the upper yield strength. Nitrogen is probably the responsible interstitial element. Cottrell's classical three stage experiment will be duplicated on a third tensile specimen of composition NASV-11 to verify the proposed explanation. These stages include (1) stressing the specimen until the

TABLE 14 - Diamond Pyramid Hardness^a Data for Composition NASV-15
(Ta-9W-1.5Re-1Hf-0.03N)

Condition	Hardness
As-Cast	370
As-Extruded	398
Extruded Plus 2 hours at 2000°C plus 2 hours at 1400°C	360
As-Swaged (83% Red.)	446

a. 30 Kg Load

TABLE 15 - Chemical Analysis of Composition NASV-15
(Ta-9W-1.5Re-1Hf-0.03N)*

Type of Sample	Position	Analysis (Weight Percent)			
		W	Re	Hf	N
Chips	Top	--	--	--	0.024
Chips	Bottom	9.3	1.45	1.07	0.029

* 0.06% N intentionally added to electrode.

TABLE 16 - Room Temperature Tensile Data^a on Composition NASV-11(b)
(Ta-9W-1.5Re-1Hf-0.015C-0.015N)

Test	Yield Strength			Ultimate Tensile Strength (psi)	% Elongation		Percent Reduction in Area
	Upper (psi)	Lower (psi)	0.2% Offset (psi)		Uniform	Total	
Initial Test	145,600	134,400	145,800	140,800	13.4	32.1	77.3
ReTest	149,600	136,300	143,000	141,500	14.1	31.4	76.9

- a. 0.005 in/in/min to 0.6% yield and then 0.05 in/in/min to fracture.
b. Specimens annealed for one hour at 1650°C(3000°F) prior to test.

drop in yield strength occurs, (2) immediately restressing the specimen to show the absence of the yield point, and (3) restressing the specimen after aging to show the return of the yield point.

D. PHASE IDENTIFICATION AND MORPHOLOGY

During the quarter, further work was done to more precisely define the position of the phase boundaries within the tantalum rich corner of the 1315°C (2400°F) isotherm of the (Ta-W)-Hf-C phase diagram, as previously proposed.² Dispersed phases were extracted from two creep specimens, one each of two compositions, both of which lie near the somewhat poorly defined boundary between the three phase matrix-Ta₂C-HfC region and the two phase matrix-HfC region. The first specimen, of composition NASV-5 (Ta-9.6W-3.15Hf-0.05C), had been annealed for 1 hour at 1650°C (3000°F) and tested in creep for 79 hours at 1315°C (2400°F) under an applied stress of 15,000 psi. The second, of composition NASV-6 (Ta-9.6W-3.9Hf-0.1C), had been similarly annealed and tested in creep for 41.4 hours under the same conditions of temperature and stress. X-ray diffraction analyses indicated that each residue was composed of approximately equal quantities of the same two FCC phases, having lattice parameters of 4.57 Å and 4.60 to 4.61 Å respectively. One of the phases was undoubtedly HfC with some substitution of Ta for the Hf as indicated by x-ray fluorescence data. The HfC also appeared to have a carbon deficiency. The second phase is believed to be an anomalous hafnium oxycarbide, similar to those observed in the Zr-C-O system by Henney and Jones¹⁰ and in the Cb-Zr-C system by Cornie, et al.¹¹ Which of the two phases is the monocarbide and which is the oxycarbide is not clear. However, as no Ta₂C was observed, both compositions were assumed to be within the two phase matrix-HfC region of the isotherm, and are so indicated in Figure 13.

Previously obtained data on compositions NAS-7 (Ta-8.2W-1Hf-0.07C) and NAS-8 (Ta-8.2W-1Hf-0.10C) are also included in Figure 13 to better define the boundary between the two phase matrix-Ta₂C region and the three phase matrix-Ta₂C-HfC region. With the exception of a minor amount of HfO₂, the only phase indicated in either material was the HCP tantalum dimetal carbide.

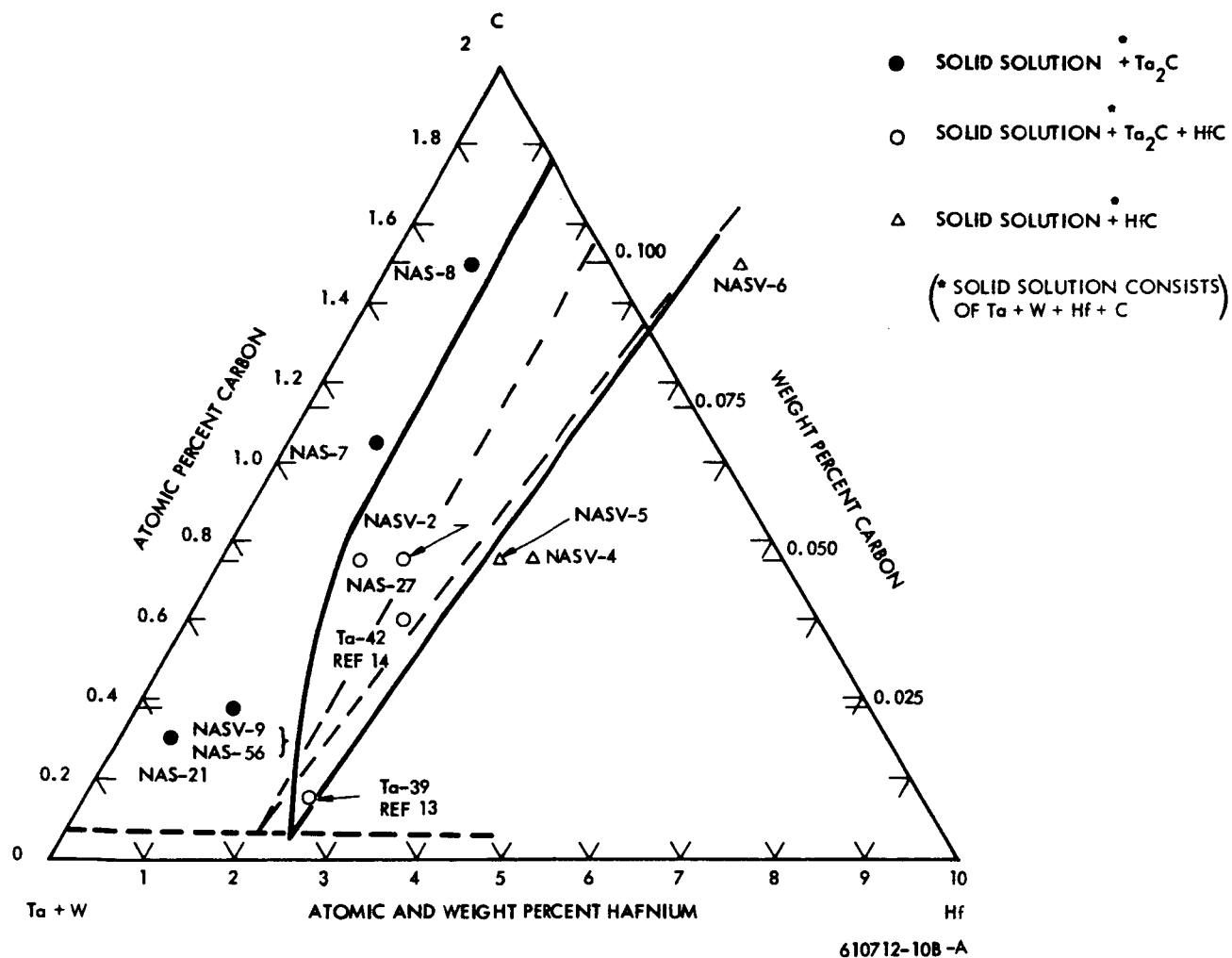


FIGURE 13 - Tantalum Rich Corner of the 1315°C (2400°F) Isotherm of the (Ta+W)-Hf-C Pseudo Ternary Phase Diagram

The proposed phase diagram was also compared with that published by Rudy on the Ta-Hf-C system,¹² for which he presents isotherms from 1000°C (1830°F) through 3980°C (7195°F). Superimposed on Figure 13, in dotted lines, are the phase boundaries obtained by graphic extrapolation of Rudy's data from the various isotherms, and corrected for the exaggerated carbon content at the intersection of the four phase regions.

It appears that the main effect of the tungsten is to shift the intersection of the four phase-fields towards the Ta-C edge of the diagram. As this intersection is presently defined by a single data point (i. e. , Ta-39), this sample is being re-evaluated for its carbon content and its contained phases. Little or no effect on the boundary separating the three phase and two phase matrix-HfC regions was observed.

The identity of phases existing in compositions NASV-10, 11, and 15 were determined after 500 hour aging heat treatments at 1250°C (2280°F) in a vacuum of 10^{-9} torr. The results of x-ray diffraction analyses of the chemically extracted phases are listed in Table 17. Starting with the least complex system, the only existing phase in either of the two aged samples of composition NASV-15, other than minor amounts of undissolved BCC tantalum matrix and monoclinic ZrO_2 , was the FCC phase, HfN. A comparison of the measured lattice parameter, a_o , of 4.525 Å with the published value of 4.52 Å* for HfN indicates little or no substitution of Ta or W for Hf.

The phases existing in the extracted residue of the NASV-10 sample consisted of a trace of ZrO_2 and larger amounts of undissolved BCC tantalum matrix and a FCC phase, believed to be (Zr,Hf)N as ZrN and HfN are isomorphs. A fluorescence analysis of the residue indicated that the ratio of Zr to Hf in the residue was essentially the same as the 1 to 1 atomic ratio of the two elements added to the alloy. The lattice parameter, a_o , of the (Zr,Hf)N was 4.56 Å compared to 4.52 Å for HfN* and 4.56 Å for ZrN**, indicating a

* ASTM card No. 6-0516 for HfN.

** ASTM card No. 2-0956 for ZrN.

**TABLE 17 - X-ray Diffraction Analyses on Extracted Residues from
Compositions NASV-10, NASV-11, and NASV-15**

Composition	Condition	Phases	Lattice Parameters (Å)
Ta-7.1W-1.56Re -0.25Hf-0.13Zr -0.03N (NASV-10)	As-Forged + 2 hrs. at 1800°C/3270°F + 500 hrs. at 1250°C/2280°F	FCC (Zr,Hf)N	4.56
		BCC Ta	3.28
Ta-9W-1.5Re-1Hf -0.015C-0.015N (NASV-11)	As-Forged + 500 hrs. at 1250°C/2280°F	FCC Hf(C,N)	4.58
Ta-9W-1.5Re-1Hf- 0.03N- (NASV-15)	As-cast + 500 hrs. at 1250°C/2280°F	FCC HfN	4.525
		BCC Ta	3.285
	As-cast + 2 hrs. at 1800°C/3270°F + 500 hrs. at 1250°C/2280°F	FCC HfN	4.525
		BCC Ta	3.285

possible nitrogen deficiency. Essentially identical results were found in a creep specimen of composition NASV-10, which had been reduced 76%, annealed for 1 hour at 1650°C (3000°F), and then tested for 140 hours at 1315°C (2400°F) under an applied stress of 20,000 psi. The lattice parameter of the FCC phase was 4.57 Å. A larger amount of monoclinic HfO₂ was also present in the creep specimen.

Finally, the FCC phase found in the sample of composition NASV-11 is believed to be the carbo-nitride of hafnium, Hf(C,N). A comparison of its lattice parameter of 4.58 Å with those of 4.52 Å and 4.641 Å for HfN and HfC*, respectively, suggest that approximately equal atomic amounts of carbon and nitrogen are present.

*ASTM card No. 9-368 for HfC.

III. FUTURE WORK

During the next quarterly period it is planned to accomplish the following:

1. Complete the generation and analysis of data for the optimization compositions.
2. Continue to process NASV-20 to 0.040 inch sheet and evaluate its weldability creep resistance, and fabricability characteristics.
3. Establish the composition for the second 4 inch diameter optimized composition and start assembly of the first melt electrode.
4. Continue phase identification and morphology studies in detail on NASV-20

IV. REFERENCES

1. R. W. Buckman, Jr. and R. T. Begley, "Development of Dispersion Strengthened Tantalum Base Alloy", Final Technical Report, Phase I, WANL-PR-(Q)-004.
2. R. W. Buckman, Jr. and R. C. Goodspeed, "Development of Dispersion Strengthened Tantalum Base Alloy", Sixth Quarterly Report, WANL-PR-(Q)-007.
3. R. W. Buckman, Jr., "Development of Dispersion Strengthened Tantalum Base Alloy", Fourth Quarterly Report, WANL-PR-(Q)-005.
4. O. D. Sherby, Acta Met., Vol. 10, 1962, p. 135.
5. R. W. Buckman, Jr., "Development of Dispersion Strengthened Tantalum Base Alloy", Fifth Quarterly Report, WANL-PR-(Q)-006.
6. R. T. Begley, W. N. Platte, R. L. Ammon, and A. I. Lewis, "Development of Niobium-Base Alloys", WADC-TR-57-344, Part V, January, 1961.
7. E. Rudy and H. Nowotny, "Untersuchen in System Hafnium-Tantal-Kohlenstoff", Mh. Chemie, 94, pp. 507-517, 1963.
8. E. K. Storms, "A Critical Review of Refractories - Part I - Selected Properties of Group 4a, 5a, and 6a Carbides", LAMS-2674 (Part I), 1962.
9. A. H. Cottrell, Dislocations and Plastic Flow in Crystals, Oxford University Press, 1953.
10. J. Henney and J. W. S. Jones, "Ternary Phases in the Zirconium-Carbon-Oxygen System", AERE-R 4619.
11. J. Cornie, E. Delgrosso, and R. Granger, "Phase Diagram of the Columbium-Zirconium-Carbon System at 1538°C and 1092°C", PWAC-461, 1965.
12. E. Rudy, "Ternary Phase Equilibria in Transition Metal-Boron-Carbon-Silicon Systems", Part II - Ternary Systems, Vol. 1 - Ta-Hf-C System, AFML-TR-65-2 (Part II, Vol. I).
13. R. L. Ammon and A. M. Filippi, "Pilot Production and Evaluation of Tantalum Alloy Sheet", Quarterly Report No. 9, WANL-PR-M-011.

APPENDIX I

Compositions of alloys discussed in this report are listed below:

Consumable Electrode Melted (2 Inch Diameter Ingots)

<u>Heat Number</u>	<u>Composition Weight Percent</u>
NASV-2	Ta-8W-2Hf-0.05C
NASV-4	Ta-8W-2.7Hf-0.4Zr-0.05C
NASV-5	Ta-9.6W-3.15Hf-0.05C
NASV-6	Ta-9.6W-3.90Hf-0.10C
NASV-7	Ta-5.7W-1.56Re-0.7Mo-0.25Hf-0.13Zr-0.015N-0.015C
NASV-8	Ta-5.7W-1.56Re-0.7Mo-0.75Hf-0.13Zr-0.015N-0.015C
NASV-9	Ta-9W-1Hf-0.025C
NASV-10	Ta-7.1W-1.56Re-0.25Hf-0.12Zr-0.03N
NASV-11	Ta-9W-1.5Re-1Hf-0.015C-0.015N
NASV-12	Ta-7.5W-1.5Re-0.5Hf-0.015C-0.015N
NASV-13	Ta-6.5W-2.5Re-0.3Hf-0.01C-0.01N
NASV-14	Ta-4W-1Mo-2Re-0.3Zr-0.015C-0.015N
NASV-15	Ta-9W-1.5Re-1Hf-0.06N
NASV-16	Ta-9.5W-0.5Re-0.25Zr-0.02C-0.01N
NASV-17	Ta-4W-3Re-0.75Hf-0.01C-0.02N
NASV-18	Ta-5W-1Re-0.3Zr-0.02N
T-333 (NASV-20)*	Ta-8W-1Re-0.7Hf-0.025C

Non-Consumable Electrode Melted (800 Gram Ingots)

NAS-7	Ta-8.2W-1Hf-0.07C
NAS-8	Ta-8.2W-1Hf-0.10C
NAS-21	Ta-8.6W-0.53Hf-0.02C
NAS-27	Ta-4.6W-1.5Hf-0.05C
NAS-36	Ta-5.7W-1.56Re-0.7Mo-0.25Hf-0.13Zr-0.015C-0.015N
NAS-56-57	Ta-8W-1Re-0.7Hf-0.025C

*4 Inch Diameter Ingot.

APPENDIX II

NASV-20 (Ta-8W-1R-0.7Hf-0.025C)
As-Cast

<u>d</u>	<u>Intensity</u>	<u>Phase</u>
2.68	M	HCP
2.58	VW	?
2.45	M	HCP
2.33	VS	BCC
1.82	M	HCP
1.645	MS	BCC
1.55	M	HCP
1.40	M	HCP
1.345	MS	BCC
1.31	M	HCP
1.29	M	HCP
1.225	VW	HCP
1.165	M	BCC
1.040	MS	HCP-BCC
0.992	W	HCP
0.965	VW	HCP
0.951	W	BCC
0.881	S	BCC
0.863	W	HCP
0.840	W	HCP
0.824	W	BCC
0.7772	MS	BCC
0.776	MS	HCP

NOTE: HCP $a_o = 3.10 \text{ \AA}$;
 $c_o = 4.92 \text{ \AA}$;
 $c/a = 1.59$
 assumed to be Ta_2C
 BCC $a_o = 3.29 \text{ \AA}$
 assumed to be Ta-W-Hf

NASV-5 (Ta-9.6W-3.15Hf-0.05C)
Creep Specimen (NASV-5-2C)

<u>d</u>	<u>Intensity</u>	<u>Phase</u>
2.93	VW	$\beta(2.65)$
2.65	VS	FCC ₁ ; FCC ₂
2.54	VW	$\beta(2.54)$
2.29	VS	FCC ₁ ; FCC ₂
1.80	VW	$\beta(1.62)$
1.62	S	FCC ₁ ; FCC ₂
1.54	VW	$\beta(1.384)$
1.384	S	FCC ₁ ; FCC ₂
1.325	M	FCC ₁ ; FCC ₂
1.148	W	FCC ₁ ; FCC ₂
1.055	M	FCC ₁
1.050	M	FCC ₂
1.030	M	FCC ₁
1.023	M	FCC ₂
0.940	M	FCC ₁
0.933	M	FCC ₂
0.887	M	FCC ₁
0.880	M	FCC ₂
0.814	W	FCC ₁
0.809	W	FCC ₂
0.7785	M	FCC ₁

NOTE: FCC₁ $a_o = 4.61 \text{ \AA}$;
 FCC₂ $a_o = 4.57 \text{ \AA}$
 assumed to be $(Hf,Ta)C_{1-x}$
 and $(Hf,Ta)(C,O)$

NASV-6 (Ta-9.6W-3.90Hf-0.10C)
Creep Specimen (NASV-6-2C)

<u>d</u>	<u>Intensity</u>	<u>Phase</u>
2.92	VW	$\beta(2.64)$
2.64	VS	FCC ₁ ; FCC ₂
2.53	VW	$\beta(2.28)$
2.45	VVW	?
2.28	VS	FCC ₁ ; FCC ₂
2.10	VVW	?
1.79	VW	$\beta(1.62)$
1.62	S	FCC ₁ ; FCC ₂
1.53	VVW	?
1.38	S	FCC ₁ ; FCC ₂
1.32	M	FCC ₁ ; FCC ₂
1.150	W	FCC ₁
1.143	W	FCC ₂
1.055	M	FCC ₁
1.058	M	FCC ₂
1.029	M	FCC ₁
1.022	M	FCC ₂
0.939	M	FCC ₁
0.932	M	FCC ₂
0.886	M	FCC ₁
0.879	M	FCC ₂
0.814	W	FCC ₁
0.808	W	FCC ₂
0.778	M	FCC ₁
0.774	W	FCC ₂

NOTE: FCC₁ $a_o = 4.60 \text{ \AA}$
 FCC₂ $a_o = 4.57 \text{ \AA}$
 assumed to be (Hf,Ta)C_{1-x}
 and (Hf,Ta) (C,O)

NASV-15 (Ta-9W-1.5Re-1Hf-0.06N)
As-cast; Aged for 500 hrs/1250°C(2280°F)

<u>d</u>	<u>Intensity</u>	<u>Phase</u>
3.15	W	HfO ₂
2.90	W	$\beta(2.62)$
2.80	W	HfO ₂
2.62	VS	FCC
2.50	W	HfO ₂
2.32	S	BCC
2.26	S	FCC
1.64	M	BCC
1.60	MS	FCC
1.365	MS	FCC
1.34	MS	BCC
1.308	M	FCC
1.16	M	BCC
1.132	M	FCC
1.038	MS	FCC, BCC
1.013	MS	FCC
0.948	W	BCC
0.925	M	FCC
0.878	M	BCC
0.873	M	FCC
0.822	W	BCC
0.802	W	FCC
0.775	M	BCC

NOTE: FCC $a_o = 4.525 \text{ \AA}$
 assumed to be HfN
 BCC $a_o = 3.285 \text{ \AA}$
 assumed to be alloy matrix

NASV-15 (Ta-9W-1.5Re-1Hf-0.06N).
Solution heat treated for 2 hrs./1800°C
(3270°F); aged for 500 hrs./1250°C
(2280°F).

<u>d</u>	<u>Intensity</u>	<u>Phase</u>
3.15	VW	HfO ₂
2.90	VW	β(2.62)
2.80	VW	HfO ₂
2.62	VS	FCC
2.50	VW	HfO ₂
2.32	S	BCC
2.26	S	FCC
2.00	W	HfO ₂
1.64	M	BCC
1.60	S	FCC
1.365	S	FCC
1.337	MS	BCC
1.308	M	FCC
1.160	MW	BCC
1.132	MW	FCC
1.038	MS	FCC, BCC
1.013	MS	FCC
0.948	W	BCC
0.925	M	FCC
0.878	M	BCC
0.873	M	FCC
0.822	W	BCC
0.802	W	FCC
0.775	M	BCC

NOTE: FCC $a_o = 4.525 \text{ \AA}$
assumed to be HfN
BCC $a_o = 3.285 \text{ \AA}$
assumed to be alloy matrix

NASV-10 (Ta-7.1W-1.56Re-0.25Hf-
0.12Zr-0.03N). Solution heat treated for
2 hrs./1800°C (3270°F); aged for 500 hrs./
1250°C (2280°F).

<u>d</u>	<u>Intensity</u>	<u>Phase</u>
3.15	W	HfO ₂
2.82	W	HfO ₂
2.63	M	FCC
2.33	S	BCC
2.27	M	FCC
1.642	M	BCC
1.610	M	FCC
1.375	M	FCC
1.340	MS	BCC
1.315	W	FCC
1.162	MW	BCC
1.140	W	FCC
1.047	W	FCC
1.038	M	BCC
1.020	W	FCC
0.948	W	BCC
0.932	W	FCC
0.878	S	FCC, BCC
0.822	VW	BCC
0.808	VW	FCC
0.775	M	FCC, BCC

NOTE: FCC $a_o = 4.56 \text{ \AA}$
assumed to be (Zr,Hf)N_{1-x}
BCC $a_o = 3.28 \text{ \AA}$
assumed to be alloy matrix

NASV-10 (Ta-7.1W-1.56Re-0.25Hf-0.12Zr-0.03N) Creep specimen (NASV-10B-1C).

<u>d</u>	<u>Intensity</u>	<u>Phase</u>
3.15	M	HfO ₂
2.92	M	?
2.82	M	HfO ₂
2.63	S	FCC
2.52	W	HfO ₂
2.32	W	HfO ₂
2.28	S	FCC
1.84	W	HfO ₂
1.81	W	HfO ₂
1.68	W	HfO ₂
1.65	W	HfO ₂
1.615	MS	FCC
1.57	W	HfO ₂
1.52	W	HfO ₂
1.375	MS	FCC
1.34	W	HfO ₂
1.319	M	FCC
1.142	MW	FCC
1.048	MS	FCC
1.022	MS	FCC
0.932	MS	FCC
0.870	MS	FCC
0.8085	M	FCC
0.773	M	FCC

NOTE: FCC $a_o = 4.57 \text{ \AA}$
assumed to be (Zr,Hf)N_{1-x}

NASV-11 (Ta-9W-1.5Re-1Hf-0.015C-0.015N) Solution heat treated for 2 hrs./1800°C (3270°F); aged for 500 hrs./1250°C (2280°F).

<u>d</u>	<u>Intensity</u>	<u>Phase</u>
3.15	VW	HfO ₂
2.93	VW	$\beta(2.64)$
2.81	VW	HfO ₂
2.64	VS	FCC
2.52	VW	HfO ₂
2.28	S	FCC
2.00	W	HfO ₂
1.62	MS	FCC
1.38	MS	FCC
1.34	W	BCC
1.32	M	FCC
1.165	VW	BCC
1.145	MW	FCC
1.050	M	FCC
1.040	VW	BCC
1.024	M	FCC
0.935	M	FCC
0.882	M	FCC
0.810	MW	FCC
0.7745	M	FCC

NOTE: FCC $a_o = 4.58 \text{ \AA}$
assumed to be Hf(C,N)
BCC $a_o = 3.29 \text{ \AA}$
assumed to be alloy matrix